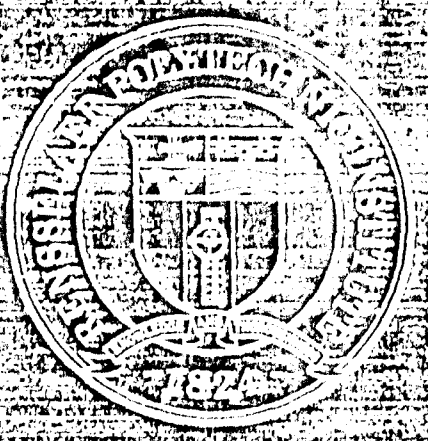

Rensselaer Polytechnic Institute

Troy, New York 12180

2

AFOSR-TR- 88-0910

CE-Report No. CE-88-02

SMALL STRAIN RESPONSE OF RANDOM ARRAYS OF ELASTIC SPHERES USING A NONLINEAR DISTINCT ELEMENT PROCEDURE

by

E. Petrakis, R. Dobry and T. Ng

Prepared under Grant AFOSR-86-0135
United States Air Force
Office of Scientific Research
Bolling Air Force Base, Washington, DC 20332-6448

Department of Civil Engineering
Rensselaer Polytechnic Institute
Troy, NY 12180-3590

July 1988

UNCLASSIFIED

SECURITY CLASSIFICATION OF THIS PAGE

REPORT DOCUMENTATION PAGE

1a. REPORT SECURITY CLASSIFICATION: UNCLASSIFIED	1b. RESTRICTIVE MARKINGS
2a. SECURITY CLASSIFICATION AUTHORITY	3. DISTRIBUTION/AVAILABILITY OF REPORT: Approved for Public Release; Distribution Unlimited
2b. DECLASSIFICATION/DOWNGRADING SCHEDULE	
4. PERFORMING ORGANIZATION REPORT NUMBER(S): CE-88-02	5. MONITORING ORGANIZATION REPORT NUMBER(S): AFOSR-TR- 88-0910
6a. NAME OF PERFORMING ORGANIZATION: Rensselaer Polytechnic Institute; 6b. OFFICE SYMBOL (If applicable): N/A	7a. NAME OF MONITORING ORGANIZATION: AFOSR/NA
6c. ADDRESS (City, State and ZIP Code): Department of Civil Engineering R.P.I., Troy, N.Y. 12180-3590	7b. ADDRESS (City, State and ZIP Code): Bldg. 410 Bolling AFB, DC 20332-6448
8a. NAME OF FUNDING/SPONSORING ORGANIZATION: AFOSR; 8b. OFFICE SYMBOL (If applicable): N A	9. PROCUREMENT INSTRUMENT IDENTIFICATION NUMBER: SFR CONTRACT AFOSR 86-0135
8c. ADDRESS (City, State and ZIP Code): Bldg. 410 Bolling AFOSR, DC 20332-6448	10. SOURCE OF FUNDING NOS. — PROGRAM ELEMENT NO.: 6.1102F; PROJECT NO.: 2302; TASK NO.: C1; WORK UNIT NO.:
11. TITLE (Include Security Classification): (U) Small Strain Response of Random Arrays of Elastic Spheres Using a Nonlinear Distinct Element Procedure	
12. PERSONAL AUTHOR(S): Emmanuel Petrakis, Ricardo Dobry, Tang-Tat Ng	
13a. TYPE OF REPORT: ANNUAL; 13b. TIME COVERED: FROM 87/05/06 TO 88/05/05; 14. DATE OF REPORT (Yr., Mo., Day): July 1988; 15. PAGE COUNT: 59	
16. SUPPLEMENTARY NOTATION	
17. COSATI CODES — FIELD / GROUP / SUB. GR.	18. SUBJECT TERMS (Continue on reverse if necessary and identify by block number): Particulate Mechanics, Random Arrays of Spheres, Contact Mechanics, Distinct Element Method, Isotropy, Anisotropy, Small Strain, Wave Velocity,

19. ABSTRACT (Continue on reverse if necessary and identify by block number)

Granular soil is represented in this work by 2-D random arrays of elastic, rough, quartz spheres using the "distinct element" method. The original 3-D computer code TRUBAL, originally developed by Peter Cundall, has been modified at RPI by the introduction of a general solution to the Hertz-Mindlin contact problem. This was achieved by attaching a subroutine to the original code, which describes the nonlinear force-displacement relationship at the intergranular contacts, by means of plasticity theory and kinematic hardening. The above modified program (CONBAL-2) developed as part of another RPI project, can perform 2-D simulations and has already been used to study the dynamic small strain behavior as well as the large strain behavior of sand. The 2-D small strain simulations presented in this report include determination of compressional wave propagation velocities for random arrays isotropically and anisotropically loaded, and the results are compared, with excellent agreement, to existing analytical and numerical results as well as to experiments performed

(Continued)

20. DISTRIBUTION/AVAILABILITY OF ABSTRACT: UNCLASSIFIED/UNLIMITED ☒ SAME AS RPT. ☐ OTIC USERS ☐	21. ABSTRACT SECURITY CLASSIFICATION: UNCLASSIFIED
22a. NAME OF RESPONSIBLE INDIVIDUAL: Major Steven C. Boyce	22b. TELEPHONE NUMBER (Include Area Code): (202)767-6963; 22c. OFFICE SYMBOL: AFOSR/NA

DD FORM 1473, 83 APR EDITION OF 1 JAN 73 IS OBSOLETE.

UNCLASSIFIED

SECURITY CLASSIFICATION OF THIS PAGE

on the large triaxial cubical specimen at the Univesity of Texas. It is found that the fabric of the material plays a very important role in the above phenomena. In all stages of the simulations, the observed macroscopic phenomena are related to the microscopic phenomena at the interparticle contact level.

TABLE OF CONTENTS

page

Abstract i

Introduction 1

Random Arrays and the Distinct Element Method 6

Numerical Simulations of the Small Strain Behavior of Quartz Sand 11

i) Isotropically Compressed Random Arrays of Spheres . 12

ii)Anisotropically Compressed Random Arrays of Spheres 18

Conclusion 30

References 32

Tables and Figures 37

ABSTRACT

Granular soil is represented in this work by 2-D random arrays of elastic, rough, quartz spheres using the "distinct element" method. The 3-D computer code TRUBAL, originally developed by Peter Cundall, has been modified at RPI by the introduction of a general solution to the Hertz-Mindlin contact problem. This has been achieved by attaching a subroutine to the original code, which describes the nonlinear force-displacement relationship at the intergranular contacts, by means of plasticity theory and kinematic hardening. The above modified program (CONBAL-2), developed as part of another RPI project, can perform 2-D simulations and has already been used to study the dynamic small strain behavior as well as the large strain behavior of sand. The 2-D small strain simulations in this report include the determination of compressional wave velocities for isotropically and anisotropically loaded random arrays of spheres. The results are compared with excellent agreement to existing analytical and numerical solutions, as well as to experiments performed on the large triaxial cubical specimen at the University of Texas. It is found that the fabric of the material plays a very important role in the above phenomena. In all stages of the simulations, the observed macroscopic phenomena are related to the microscopic phenomena at the interparticle contact level.

INTRODUCTION

Since the early 1960's, a large number of experimental studies has been performed on the small strain behavior of sand aiming at providing empirical correlations for practical use (Hardin and Richart, 1963, Hardin and Black, 1966, Drnevich and Richart, 1970, Dobry et al, 1982). The equations relating the shear modulus, G_{max}, to the void ratio, e, and the effective confining pressure, $\bar{\sigma}_o$, proposed by Hardin and Richart (1963), Seed and Idriss (1970) and Seed et al (1984) are especially important to this report. These empirical relationships are based on the assumption that the soil can be treated as an elastic, isotropic solid. In all three correlations:

$$G_{max} = A\, f(e)\, \bar{\sigma}_o^p \qquad (1)$$

where A is a constant, f(e) is an experimentally defined function of the void ratio, e, $\bar{\sigma}_o = 1/3(\bar{\sigma}_1 + \bar{\sigma}_2 + \bar{\sigma}_3)$ is the mean effective stress, and p is an experimentally defined exponent which has been found to be approximately 0.5. The above empirical relations assume that the value of G_{max} (and thus, the wave velocity, $V_s = \sqrt{G_{max}/\rho}$, where ρ is the mass density of the soil), is the same for isotropically and anisotropically loaded sand, provided that the effective mean stress, $\bar{\sigma}_o$, is the same. Furthermore, all correlations assume

that for the anisotropic loading case, G_{max} and V_s do not change in direction.

These assumptions for G_{max} in sands have been challenged by the experimental results obtained by Schmertmann (1978), Roesler (1979), Knox et al (1982), and Yu and Richart (1984). It was established by these researchers that both the compressional, V_p, and shear, V_s, wave velocities depend on the stresses in the direction of wave propagation and particle motion polarization, and not on the effective mean stress.

Stokoe et al (1980) developed at the University of Texas at Austin a large scale, 7 X 7 X 7 ft cubical triaxial facility for the specific purpose of measuring V_s and V_p in dry sand. In this facility, a triaxial state of stress, $\sigma_1 \neq \sigma_2 \neq \sigma_3$ ($\sigma=\bar{\sigma}$ in dry sand) can be achieved. All tests performed to date at the University of Texas have used a locally found, medium to fine, washed mortar sand classified as SP, with effective grain size, D_{10}=0.28 mm and a uniformity coefficient, C_u, of 1.7. The sand is placed by the raining technique and tested dry. The values of the principal stresses have ranged between 15 psi and 40 psi, with the stress ratio, $K = \sigma_1/\sigma_3 = 1$ to 2.67. Kopperman et al (1982) used this facility to study the effect of the stresses on the propagation velocity of compressional waves, V_p. They caused P-waves to propagate along one of the

principal stresses (σ_a), while varying the others; they concluded that:

$$V_p = L\ \sigma_a^m \text{ (fps)} \tag{2}$$

where L ≃ 220 to 290 and m ≃ 0.20 to 0.24 are experimentally defined constants. The sensitivity of V_p on σ_a and its insensitivity to variations in the other two principal stresses, σ_b and σ_c perpendicular to wave propagation is illustrated in Fig. 1.

In a similar way, Knox et al (1982) studied the propagation of shear waves under anisotropic conditions and concluded that:

$$V_s = F\ \sigma_a^{ma}\ \sigma_b^{mb}\ \sigma_c^{mc} \text{ (fps)} \tag{3}$$

where F is a constant, ma ≃ mb ≃ 0.09 to 0.12, and mc ≃ 0 to 0.01. Thus, in these two cases the experimental findings of Schmertmann (1978) and Roesler (1979) were confirmed, and it was established that empirical correlations, such as Eq. 1, do not adequately describe the behavior of anisotropically loaded sand, and they need to be revised and upgraded. In most cases sand is anisotropically loaded, and more than 2 elastic constants may be needed. For example, if $\sigma_1 = \sigma_2 \neq \sigma_3$, the soil

will behave as a transversely isotropic medium and 5 constants (moduli) will be needed; in the more general case of $\sigma_1 \neq \sigma_2 \neq \sigma_3$, the sand may behave as an orthotropic continuum and at least 9 constants may be required (Sokolnikoff, 1956).

This contradiction between the early and the more recent laboratory data indicates that the constitutive modelling phenomenon of soils at small strains is more complex than originally anticipated. While it is true that a number of phenomenological continuum models of the small strain (elastic) response of sand have been proposed (Rowe, 1971, Coon and Evans 1971, Lade and Nelson, 1988), they apply only to isotropic sands. On the other hand, experimental studies by Oda (1974), Oda and Konishi (1974) , Oda et al (1983, 1985) have indicated the potential of a particulate mechanics approach to explain the observed behavior. This is further strengthened by the findings of earlier analytical work by Duffy and Mindlin (1957), Deresiewicz (1958a), Duffy (1959), and others. Consequently, it is generally accepted that at small strains the behavior of a granular medium is governed by the elasticity of the particles (i.e. the force-displacement nonlinearity at the interparticle contacts), while in the very large strain range the geometrical arrangement and the kinematics of the particles become dominant.

Although a number of analytical, experimental and numerical particulate mechanics studies have been performed in the past on regular and random arrays of spheres, their scope has been limited by the available computer capabilities and the lack of a realistic force-deformation law at the intergranular contacts. In the last few years the wider availability of supercomputers for basic engineering research and the development, at RPI, of a general solution to the Hertz-Mindlin problem at the contact between two identical elastic, rough spheres (Seridi and Dobry, 1984, Dobry et al, 1988) have significantly improved the situation. This solution, coded as program CONTACT, could now be used as a subroutine in a finite element program which describes the stress-strain response of granular soil. This was done as part of the current AFOSR sponsored research, and Petrakis and Dobry (1987, 1988a, 1988b) used the above relationship in a nonlinear finite element scheme to succesfully predict the stress-strain response of a regular/random array of equal spheres.

RANDOM ARRAYS AND THE DISTINCT ELEMENT METHOD

Several approaches have been used to model the effect of randomness and deviations from regularity in arrays of equal or unequal spheres. Serrano and Rodrigues-Ortiz (1973) suggested a method for generating a random configuration of unequal disks or spheres having a prescribed grain size distribution. Cundall and Strack (1979) used a similar approach in conjuction with their "distinct element method" to succesfully simulate the mechanical response of arrays and disks and spheres under a variety of loading conditions. In their method, an explicit finite difference formulation is used to determine the static response of the array to applied strains (program TRUBAL) or to a boundary displacement (program BALL).

TRUBAL uses a periodic space in a form of a cube (3-D) or square (2-D), such as that of Fig. 2, to minimize the effect of the boundaries and allow the use of a relatively small number of particles. A uniform strain field is applied to all particles and the corresponding contact forces are calculated from the relative displacements between neighboring spheres. Initially, the program used an arbitrary, linear, non pressure dependent law to describe the force-deformation behavior at each interparticle cointact; in a later version of the program (Zhang and Cundall, 1986) a linear pressure dependent

force-deformation relationship was introduced. As illustrated by Fig. 3, these contact forces, P_i, produce in each sphere a resultant unbalanced force, ΣP_i , and unbalanced moment, ΣM_i, which induce linear and angular accelerations in the particle. These accelerations are used in turn to compute a new particle position at the end of a time increment, Δt, and new contact forces. The process is repeated until static equilibrium is achieved ($\Sigma M_i \simeq \Sigma P_i \simeq 0$). The method has the advantage of decreasing substantially the required computer memory, as no large stiffness matrices need to be calculated and inverted. However, the execution time is large due to the great number of iterations needed to assure static equilibrium.

Cundall and Strack (1979), Strack and Cundall (1984) and Zhang and Cundall (1986) have used BALL and TRUBAL for succesful simulations of monotonic direct simple shear and compression triaxial tests.

The available program TRUBAL (Strack and Cundall, 1984) was modified at RPI by Ng and Dobry (1988) within another, NSF sponsored project, by replacing the existing arbitrary linearly elastic-perfectly plastic, non pressure dependent, force-displacement relation at the intergranular contacts, by the more realistic and rigorous Hertz-Mindlin contact law. This was accomplished by attaching the program CONTACT

described previously, as a subroutine in TRUBAL (Table 1). The new modified program was named CONBAL-2 (CONtact truBAL in 2-dimensions). CONBAL-2 is a two-dimensional version of TRUBAL which incorporates CONTACT and has also been modified to run more efficiently on the computer. Furthermore, CONBAL-2 does not allow any rotation or rolling of the particles, as this causes as yet unsolved problems in the numerical simulations. The 2-D character and lack of particle rotation in CONBAL-2 makes the array somewhat stronger than actual, 3-D random arrays and soils; Ng and Dobry (1988) have approximately corrected for this by reducing the interparticle angle of friction. Therefore, CONBAL-2 is very similar to the original program TRUBAL, except for the two differences just noted, and for the very important introduction of the effect of the normal force which is now rigorously modelled by the Hertz-Mindlin-Dobry algorithm.

The accuracy of CONBAL-2 was checked by comparing the results of a simulation of monotonic pure shear loading on an isotropically compressed simple cubic array of quartz spheres, to the rigorous solution obtained by Deresiewicz (1958). The "window" of the nine identical spheres used in the CONBAL-2 simulation appears in Figure 4. The results of the numerical simulation are plotted in Figure 4 (solid line), and are in

excellent agreement with the rigorous solution (crosses). Additional numerical simulations appear in Ng and Dobry (1988); they include a number of large strain numerical experiments on random arrays of equal or unequal quartz spheres under cyclic and static, drained and undrained conditions. The results of these simulations are in excellent agreement with comparable experimental data on granular soils reported in the literature. Moreover, CONBAL-2 has shown to have considerable predictive power. For example, Ng and Dobry (1988) subjected the 2-D array of 57 unequal spheres shown in Fig. 5, to a monotonical constant-volume uniaxial compression, after the array had been consolidated under an isotropic pressure, $\bar{\sigma}_o$, of 3.4 kgf/cm^2. This was done by increasing the vertical stress, σ_1, acting on the array, while varying the horizontal compressive stress, σ_2, as much as necessary to keep the volume constant. To model the situation during the corresponding undrained compression "triaxial" test in which the "cell pressure" would be kept constant at $\bar{\sigma}_o$=3.4 kgf/cm^2, a "pore water pressure" u=-(σ_2-3.4) was defined.

The results of this simulation are summarized in Fig. 6. The figure includes the calculated axial stress-strain curve in Fig. 6a, the variation of pore pressure, u, vs axial strain in Fig. 6b, and the effective stress path in Fig. 6c. The

behavior of the granular soil simulated is clearly dilative; it is accurately modelled by CONBAL-2, which yields results very similar to those measured in undrained triaxial tests on uniform, rounded, dense Ottawa sand, such as those of Vaid and Chern (1983) (specimen S-3), also included in Fig. 6. At first glance they may not look comparable; however, the scales are different and, with this in mind, it may be seen that the stress-strain, pore pressure-strain curves and the stress path on the $\bar{p}$-q space, are remarkably similar between specimen S-3 and the numerical simulation.

NUMERICAL SIMULATIONS OF THE SMALL STRAIN BEHAVIOR OF QUARTZ SAND

After program CONBAL-2 was checked and became ready to use, a copy was made available to this AFOSR project for research on the stress-strain behavior and development of a constitutive relation for dry granual soil.

As a first step, it was decided to start simulating phenomena in the small strain range, and at a later stage focus on the large strain, fully nonlinear inelastic behavior. Furthermore, it was also decided to compare the results of CONBAL-2 with answers obtained using the analytical and numerical procedures previously developed in this project by Petrakis and Dobry (1986, 1987), as well as with experimental data in the literature.

Random arrays of <u>equal</u> spheres were generated first, since the previous analytical and numerical methods were developed for equal spheres and much available experimental data are obtained on uniform sand. Moreover, the force-deformation relations at the interparticle contacts developed by Hertz (1882), Cattaneo (1938), Mindlin (1949) and Mindlin and Deresiewicz (1953) apply only to equal spheres of the same material; subroutine CONTACT is based on these formulations and cannot, in principle, model the contact behavior of unequal or

dissimilar spheres. Therefore, program CONBAL-2 yields rigorous results only when arrays of equal spheres are generated; however, the same program, with certain assumptions, can handle in first approximation moderately unequal spheres of the same material, provided that their diameters are not very different. In this section, results on packings of equal spheres will be presented, together with some results on an array of moderately unequal spheres.

i) Isotropically Compressed Random Arrays of Spheres

Two different 2-D random arrays of 477 identical particles having the properties of quartz (G_s= 295182 kgf/cm^2, ν_s=0.15, f=0.5, White, 1964), were generated using CONBAL-2. In the following distinct element simulations, f=0.35 was used instead of f=0.5 to correct for the effects of 2-D and absence of particle rotation as previously discussed. The first array was a very loose one, with an average coordination number, CN (number of contacts per sphere), of 2.1, while the second was medium dense with CN=3.0. It should be noted that when computing the average number of contacts per sphere in a random array, all spheres, including those with no contacts, are counted, and this causes the average coordination number to be low. These two arrays were then subjected to three different values of isotropic pressure (σ_o= 0.91, 3.34 and 6.98 kgf/cm^2),

without significant change in their average number of contacts.

The configuration of the second assemblage, with CN=3.0, and subjected to $\sigma_{11}=\sigma_{22}=\sigma_o=$ 0.91 kgf/cm^2 is shown in Fig. 7. The rectangles in this figure represent the magnitudes and directions of the contact forces; there are four different rectangle widths, each one of them corresponding to a range of forces between four equal fractions of the maximum computed contact force. For example, if the maximum contact force is F kgf, the narrowest rectangle stands for the range of forces between 0 and F/4 kgf, the next wider rectangle for the range of forces between F/4 and F/2 kgf, etc. It can be also observed that this assemblage of equal spheres has crystalized; that is, areas of regular packing appear within the random structure. This is in agreement with the experimental findings of Smith et al (1929), Bernal and Mason (1960), Bernal et al (1964), Davis and Deresiewicz (1974), Shahinpoor and Shahrpass (1982) and others, reported in Petrakis and Dobry (1986, 1988a), who proposed that a random packing of equal spheres can be represented by a combination of regular arrays. Some of these regular packings in Fig. 7 are not subjected to any contact force, with the forces being supported through arching by surrounding packings. This crystalization has lumped the array into N constituents, where N is the number of different

packings within the aggregate, and thus has increased the characteristic size of the smallest constituent. As a result, the array is not completely isotropic under isotropic stress; a much larger r mber of spheres than 477 is needed in order to have a uniform spatial distribution of the crystalized regions and achieve a statistically isotropic medium. Moreover, it can be seen in Fig. 7 that the applied stresses are mainly transmitted through columns of particles, in which all contacts along the column axis experience approximately the same contact force. These contact force directions cover a large spectrum of angles, with perhaps some preference toward the two directions parallel to the boundaries. These conclusions obtained from a visual inspection of Fig. 7 are also illustrated in Figure 8, where the frequency distribution of contact angles is shown in a polar plot together with other micromechanical statistics, such as the frequency distributions of mobilized angle (angle between contact force and contact normal), coordination number and contact force. This 477-particle packing can be approximated as isotropic under its current isotropic loading, if the effect of the orientation of the contacts along the loading directions is smoothed in Figure 8.

The two 477-particle random arrays with average coordination numbers CN=2.1 and 3.0, were subsequently used to compute the small strain shear modulus, G_{max}, under isotropic pressure. For this, both random packings were subjected to a small increment of macroscopic shear strain, $d\gamma=1X10^{-6}$, the corresponding macroscopic shear stress, $d\tau$, was calculated, and the shear modulus was computed as $G_{max}=d\tau/d\gamma$. This was done for both arrays at the three confining pressures σ_o= 0.91, 3.34 and 6.98 kgf/cm^2. The resulting shear modulus, G_{max}, has been plotted versus σ_o and the coordination number in Fig. 9, which also includes the small strain shear modulus for the simple cubic array in two dimensions (CN=4). For a given σ_o the shear modulus in Figure 9 is approximately linearly proportional to CN, similar to the analytical results reported by Yanagisawa (1983) and Petrakis and Dobry (1986, 1988a), indicating that the stiffness of a packing of spheres is controlled by both normal stress and the number of load transmitting contacts. Since most contacts have not failed in the random array of Fig. 7 (see plot of mobilized angle in Fig. 8) the whole granular assembly behaves, through its contacts, like a nonlinear truss whose stiffness is increased when new members are added. As expected, the deformation characteristics of the material of the particles control the macroscopic stress-strain response of

this granular medium under isotropic pressure, with CN being the other major factor. The same plot may also be interpreted as a plot of the shear wave velocity, V_s, versus the coordination number, CN, if it is assumed that the wave length is significantly larger than the radius of the spheres.

Figure 10 contains the above data as well as points derived by i) the Self Consistent Method (Petrakis and Dobry, 1986, 1988a); ii) analytical solutions for regular arrays; and finally, iii) the analytical expressions recently reported by Walton (1987), for random packings of equal spheres. Figure 10 is for the same three values of confining pressure, σ_o = 0.91, 3.34 and 6.98 kgf/cm^2. Walton, by considering the pressure dependent force-deformation behavior of both normal and tangential compliances at the interparticle contacts, derived the following expressions for the two elastic moduli (Lame constants), λ^* and $\mu^* = G_{max}$, of a random packing of equal elastic spheres with an infinite coefficient of friction, subjected to isotropic compression, σ_o:

$$\lambda^* = \frac{C}{10(2B + C)} \left[\frac{3\phi^2(CN)^2\sigma_o}{\pi^4 B}\right]^{1/3} \tag{4}$$

$$\mu^* = G_{max} = \frac{(5B+C)}{10(2B + C)} \left[\frac{3\phi^2(CN)^2\sigma_o}{\pi^4 B}\right]^{1/3} \tag{5}$$

$\phi=(1-n)$, where n is the average porosity of the medium, B and C are constants which depend on the material properties of the spheres, μ_s and ν_s, and CN is the average coordination number.

In Fig. 10, the points derived by the Self-Consistent Method and Eqs. 4 and 5, are the result of a three dimensional analysis, unlike the points in Fig. 9 which are for two dimensions. Since the simple cubic array appears in both plots with coordination numbers CN=4 (2-D) and CN=6 (3-D), but with the same value of shear modulus, $G_{max}=\mu^*$, it was decided to multiply the coordination number of all 2-D distinct element simulations by 6/4=1.5, to approximately "adjust" for the additional third dimension. Furthermore, since the 3-D Self Consistent Method was applied using the same value of quartz modulus for the spheres as used in the other methods, but with Poisson's ratio of the spheres, $\nu_s=0$, in order to eliminate the anisotropy inherent to the cubic arrays (Petrakis and Dobry, 1986, 1988a), Eqs 4 and 5 were modified accordingly. Specifically, for $\nu_s=0$, λ^* and C become 0 and $B=1/(2\pi\mu_s)$. The final result is the very consistent plot in Fig. 10 using points from four different methods; they essentially confirm the hypothesis presented by Yanagisawa (1983) and Petrakis and Dobry (1986) that the small strain shear modulus, G_{max}, of a random array of equal spheres is essentially a linear function

of the average number of contacts per particle. In Eq. 5 the relation between G_{max} and CN is not linear but the product of the multiplication of the two factors: porosity, n, and CN, results in an essentially linear relationship between $\mu^*=G_{max}$ and CN, once the influence of n on CN is considered.

ii)Anisotropically Compressed Random Arrays of Spheres

The same array already discussed, with 477 equal, elastic spheres and coordination number, CN=3, consolidated isotropically at $\sigma_{11} = \sigma_{22} = \sigma_o = 0.91$ kgf/cm^2 (Fig. 7) was further loaded under biaxial compression to $\sigma_{22} = 2.33$ kgf/cm^2, while keeping σ_{11} constant. The stress path appears in Fig. 11 as stress path (b). This was done to: i) investigate the influence of the magnitude and direction of the principal stresses on the velocity of longitudinal waves, V_p, propagating through this medium, ii) interpret the experimental findings of Kopperman et al (1982), and iii) verify the findings of the nonlinear finite element model presented by Petrakis and Dobry (1987, 1988b).

To compute the wave velocities, V_p, the constrained moduli $D_{ii}=V_p^2\,\rho$, were calculated first as follows: once the desired stress ratio, $K=\sigma_1/\sigma_2=\sigma_{22}/\sigma_{11}$, was reached at specific points along stress path (b) in Fig. 11, very small strain increments, $d\epsilon_{11}$, $d\epsilon_{22}$, equal to $1.062\text{X}10^{-6}$ were applied to the array with

appropriate signs. The corresponding stress increments $d\sigma_{11}$, $d\sigma_{22}$ were computed, and finally, the small strain constrained moduli $D_{ii}^{(K)}=d\sigma_{ii}/d\epsilon_{ii}$, were calculated both in the direction of the major ($\sigma_1=\sigma_{22}$) and minor ($\sigma_2=\sigma_{11}$) principal stresses. The results of these simulations are shown in Fig. 12, where the small strain constrained moduli of the random packing at every stress ratio K, $D_{ii}^{(K)}$, normalized by the constrained modulus under the initial isotropic pressure $D_{ii}^{(1)}$, are plotted against the stress ratio, $K=\sigma_{22}$ / $\sigma_{11}=\sigma_1/\sigma_2$. Figure 12 also includes data points from a number of experiments on sand performed at the University of Texas by Kopperman et al (1982), and results of the nonlinear finite element model proposed by Petrakis and Dobry (1987), all performed under analogous conditions to those of the CONBAL-2 nonlinear distinct element simulation.

The agreement between all normalized results in Figure 12, is excellent, and a straight line of equation $D_{22}^{(K)}/D_{22}^{(1)} = (\sigma_{22}/\sigma_{11})^{.38} = K^{.38}$ could be fitted to all numerical and experimental data points included in the figure. It should be noted that, if the change in sand density as K increases is neglected, $D_{22}^{(K)}/D_{22}^{(1)} = [V_p^{(K)}/V_p^{(1)}]^2$. From their experiments in sand, Kopperman et al (1982) found that Eq. 2 was applicable with $220 \leq L \leq 290$ and $m \simeq 0.2$. This gives $D_{22}^{(K)}/D_{22}^{(1)} \simeq K^{0.4}$, very similar to the line in Fig. 12. Furthermore, it was found that

the actual values of V_p calculated by CONBAL-2 for the array of Fig. 7, are within 10% of those measured by Kopperman et al (1982). Figure 12 shows that the main conclusion obtained from the University of Texas laboratory results, that the P-wave velocity ($V_p = \sqrt{D/\rho}$) propagating along a principal stress direction is only a function of that principal stress, is fully predicted by the nonlinear distinct element method. Again, this is an effect of the particulate nature of the soil, which can not be interpreted and reproduced analytically unless this particulate nature is taken into account.

Figures 13 and 14 depict the positions of the spheres, the relative magnitudes and directions of the contact forces, and the associated micromechanical statistical information, at the last stage of anisotropic loading, at $K=\sigma_{22}/\sigma_{11}=2.33/0.91=2.56$. This is the last stage of the biaxial loading simulation, whose particle configuration and micromechanical statistics under the initial isotropic pressure $\sigma_o = \sigma_{11}=\sigma_{22}=0.91$ kgf/cm^2 (K=1) was shown in Figs. 7 and 8.

Comparing the array configurations of the above two loading stages in Figs. 7 and 13, it can be seen that the array remains crystalized throughout the loading process, and that a number of the regular packings within the array remain stress free.

Similarly to Fig. 7, the four different widths of the rectangles in Fig. 13 represent the ranges of intensity of contact forces relative to the maximum contact force in each case. When the random array is subjected to isotropic pressure, the distribution of the contact forces was more or less uniform, with similar contact forces in all directions (Fig. 8). On the other hand, and as shown in Fig. 13 and 14, after the array was loaded vertically while the horizontal stress, σ_{11}, was kept constant, the number of contacts in the vertical direction increased and most of the columns transmitting loads are now essentially vertical or horizontal. These columns are similar to the "stiff chains" reported by Cundall and Strack (1983). The number of contacts in the horizontal direction has somewhat decreased, while in all other directions has decreased substantially. The magnitudes of the contact forces in the vertical contacts have also increased.

Figure 14 contains the micromechanical statistics calculated for the anisotropic stress condition of Fig. 13, including frequency distributions of contact angle, mobilized angle, coordination number and magnitude of contact force. The polar plot of frequency distribution of contact angle, quantifies the increase in the number of contacts in the vertical direction, previously discussed, as well as the

decrease of number of contacts in the other directions. Figure 14 also shows that at this point of the biaxial compression loading most contacts have failed, the particles have rearranged themselves to more stable conditions, and the distribution of coordination numbers has changed little. The polar plot of the frequency distribution of contact angle in Fig. 14 resembles a cross, with most of the contacts aligned parallel to the applied principal stresses. This is consistent with the vertical/horizontal columns transmitting loads in Fig. 13, and is different from the structure of the array under isotropic stress presented in Figs. 7 and 8. There, the frequency distributions of contact angle and contact forces were approximately uniform and few contacts had failed.

Based on the results of the numerical simulations and the above discussion, it is concluded that changes in the structure of the random packings and granular soils are responsible for the observed macroscopic behavior, and specifically for the dependence of the compressional wave velocity only on the principal stress in the direction of wave propagation. Under isotropic loading, the orientations of the contacts have a more or less uniform distribution, the material behaves isotropically and the wave propagation velocity is a function of the isotropic stress, σ_o. Under biaxial (2-D) or triaxial

(3-D) compression, a significant number of contacts is gained in the direction of the increased major principal stress, σ_1, while contacts are lost in all other directions. In the other two principal directions in which the stresses σ_2 (and σ_3) are kept constant, the number of contacts decreases, but not considerably, while many contacts are lost in all non principal directions. These contacts along principal directions form "branches" or "stiff chains" parallel to the principal stresses which transmit most of the applied principal stresses from boundary to boundary. The result is a structure reminiscent of a simple cubic array loaded by stresses σ_1, σ_2 and σ_3 parallel to the main axes of the array, and with the effect of each principal stress being uncoupled from the other two. This uncoupling, which in the simple cubic array happens naturally due to the geometry of the array, develops in the random array as a consequence of these stiff columns or "branches" of particles which carry the applied load. Therefore, as in the case of the simple cubic array (Petrakis and Dobry 1986, 1987), the longitudinal modulus, D, in any principal direction is a function only of the stress in this direction and is unaffected by variations in the stresses in the other directions. Although the CONBAL-2 runs discussed here were two dimensional, the authors postulate that the same phenomenon occurs in

three-dimensions with the formation of stiff chains in three directions instead of two. It is well known (Deresiewicz 1958) that the shear moduli of the simple cubic array depend only on two principal stresses and are independent of the third principal stress. Since the moduli of the random array are expected to be of similar nature due to the 3-D "stiff columns" just postulated, it is believed that this is the reason why the shear moduli (or S-wave velocities) have been observed to depend only on the principal stresses in the direction of wave propagation and particle motion. However, this hypothesis should be verified once the 3-D version of CONBAL-2 is developed.

To further demonstrate the fact that the P-wave propagation velocity (or the constrained modulus) is a function of the principal stress in that direction only, the same random array of 477 equal spheres was subjected to a biaxial compression-extension loading simulation under constant mean stress, σ_o=0.91 kgf/cm^2. The corresponding stress path (a) is shown in Fig. 11. The vertical stress, σ_{22}, was increased up to 1.374, while the horizontal stress σ_{11} was decreased down to 0.447 kgf/cm^2 (Fig. 15). Thus, σ_o= 1/2(1.374+0.447)=0.91 as before. Again, the normalized constrained moduli $D_{ii}^{(K)}/D_{ii}^{(1)}$, were computed at specific values of the stress ratio, $K=\sigma_{ii}/\sigma_o$,

in both directions σ_{11} and σ_{22}. Note that for any set of specific values of σ_{22} and σ_{11}, it is defined $K=\sigma_{22}/\sigma_o$ for $D_{ii}^{(K)}=D_{22}^{(K)}$, and $K=\sigma_{11}/\sigma_o$ for $D_{ii}^{(K)}=D_{11}^{(K)}$. If the moduli were a function of the mean stress (i.e if Eq. 1 were true), the P-wave propagation velocity (and the modulus) would be unaffected by the changes in the magnitude of the principal stresses. $D_{ii}^{(K)}$ would be always the same in both directions, and the plot of $D_{22}^{(K)}/D_{22}$ versus K in Fig. 16 would be a horizontal straight line. The normalized constrained moduli calculated with CONBAL-2 are plotted vs. K in Fig. 16. As σ_{22} increases, $D_{22}^{(K)}$ increases in the figure. Simultaneously, as σ_{11} decreases, $D_{11}^{(K)}$ decreases, and the plot of $D_{ii}^{(K)}/D_{ii}$ versus K follows a consistent curve valid for both directions. Therefore, Fig. 16 confirms again that the constrained moduli, D_{ii}, are affected by the principal stress in the direction of loading only and are <u>completely</u> <u>independent</u> of the mean stress. Therefore, based on the above results and those of the biaxial loading simulation (Fig. 12), it is predicted that a granular soil does not behave as a linearly elastic <u>isotropic</u> solid at small strains, but it changes its order of elastic symmetry depending on the applied principal stresses. Consequently, expressions of the type of Eq. 1 can be used only for <u>isotropically</u> consolidated soils; in all other cases, relations

of the type of Eqs. 2 and 3 should be used. The contact force distribution, formation of stiff columns and micromechanical statistics of this array at the end of the loading path (Figs. 15 and 17) are very similar to those obtained in biaxial compression under different anisotropic stress conditions (Figure 13 and 14). The crystalization appears once more; since most initial contacts have failed at this point, new have formed along the direction of the major applied principal stress. At the same time, there has been a substantial decrease in the number of contacts in the horizontal direction, and stiff columns of particles have appeared both vertically and horizontally.

Finally, in order to be able to generalize the above findings for the case of uniform random arrays of unequal quartz spheres, a random array of 531 particles of two <u>different</u> diameters was generated. This aggregate was composed of 168 spheres of radius R_1 and of 363 spheres of R_2. The ratio R_1/R_2 was set to 1.5, and thus not very different from unity, so that the Mindlin-Deresiewicz theory could be applied by using the concept of "equivalent radius". This equivalent radius, $R_e=2R_1R_2/(R_1+R_2)$, where R_1 and R_2 are the radii of the two particles in contact, has been used in the past in the case of unequal cylinders (Poritsky, 1950), and represents an

approximation to an unknown exact solution. It is derived from the Hertz (1882) theory for smooth spheres (f=0) and can be applied to the case of rough spheres as a first approximation (Ng and Dobry, 1988)

The above array was first subjected to isotropic pressure, σ_o= 1.31 kgf/cm^2; the corresponding geometric and statistical information is shown in Figs. 18 and 19. As the spheres are not identical, now there is no crystalization and the 531 sphere aggregate is almost isotropic, as can be seen from the uniform distribution of contact angles in the polar plot of Fig. 19 (compare with Fig. 8). Therefore, this 531-particle array exhibits a higher level of symmetry than the 477-sphere packing, and is taken to be isotropic. Even in this case, in which there is no crystalization, there is still a number of particles which are not in contact and do not carry any load. Moreover, when comparing this packing in Fig. 18 to the 477 equal sphere assemblage in Fig. 7, no clear system of parallel columns of particles can be detected transfering approximately the same forces across the whole array, but instead, the magnitude of the contact force varies with position.

The array was finally loaded under biaxial compression to σ_{22}=3.32 kgf/cm^2, while keeping σ_{11} constant as shown by stress path (c) in Fig. 11. The array configuration and the contact

forces at the end of the loading path are shown in Figure 20, with the corresponding micromechanical statistics presented in Fig. 21. As we can see in both figures, the contacts have been more or less eliminated in all directions except the major and minor stress directions $\sigma_1=\sigma_{22}$ and $\sigma_2=\sigma_{11}$. The number of contacts has doubled in the σ_{22} direction and has also increased more moderately in the σ_{11} direction. Most contacts have failed, and again, there are still some spheres which are not subjected to any contact force. Finally, the contact forces in this case vary again with the position of each particle. Vertical and horizontal load transmitting columns or "stiff chains" are present in Fig. 20, but they are less continuous and not so obvious as they were in the crystalized equal sphere array of Fig. 13. A close comparison between this array of unequal spheres in Fig. 20 to the equal sphere array of Fig. 13, shows that while their structures (fabrics) are fundamentally dissimilar (crystalization vs. randomness) and the distribution of forces within them very different, they both form the majority of their contacts along the directions of the applied principal stresses, when compressed biaxially. It is also interesting that the frequency distributions of the contact angle in all simulations at the end of their corresponding biaxial loading simulations (Figs. 14, 17, and

21) have the distinctive "cross" pattern with the contacts aligned along the directions of the applied principal stresses.

The normalized constrained moduli were also computed for the array of Fig. 20 at various values of the stress ratio, $K=\sigma_{22}/\sigma_{11}$, and they are plotted versus K in Fig. 22. Once more the moduli (and consequently, the P-wave velocity) are affected in first approximation by the principal stress in that direction. In addition to the results of the simulation on the unequal sphere array of Fig. 20, Fig. 22 also includes all points of Fig. 11, that is: the experimental data of Professor Stokoe and his co-workers, the nonlinear finite element results of Petrakis and Dobry (1987, 1988), and finally the results of the nonlinear distinct element method on the array of the 477 equal ~~equal~~ diameter spheres. All points are in excellent agreement, thus verifying the accuracy and versatility of the approach, and the validity of the conclusions reached for the constrained modulus, D_{ii}, and P-wave velocity, V_p, of random arrays of spheres and of granular soils.

CONCLUSION

A 2-D nonlinear distinct element simulation has been presented which interprets the behavior of granular soil at very small strains. This simulation is based on an incremental solution to the nonlinear problem of two spheres in contact (program CONTACT), incorporated into the available distinct element program TRUBAL. It has been found that this approach not only interprets succesfully the small strain behavior of granular soil, but it also provides a wealth of information on the fabric changes during loading which were until now very difficult to obtain. The results of these simulations on both isotropically and anisotropically compressed random arrays of equal and unequal spheres, are in excellent agreement with a number of previous analytical and numerical procedures, as well as with experimental data on sand in the literature. The origin of the above phenomena is the changes in the structure of the granular medium which occur when loaded, and specifically, the formation of columns of particles supporting approximately the same contact force along the directions of the applied principal stresses. Therefore, the distribution and magnitude of the contact forces are of great importance to the macroscopic response of the medium. The above phenomena, which are micromechanical in nature, can only be modelled

analytically if the particulate nature of the soil is taken into consideration and the contact forces are realistically modelled.

REFERENCES

Bernal, J.D., and Mason, J. (1960), "Coordination of Randomly Packed Spheres". Nature, Vol. 188, pp. 910-911.

Bernal, J.D., Knight, K.R. and Cherry, I, (1964), "Growth of Crystals from Random Close Packing". Nature, Vol. 202, pp. 825-854.

Cattaneo, C. (1938), "Sul Contatto di Due Corpi Elastici". Arti. Acad. Nazionale dei Lincei, Serie 6, 17, pp. 342-348, 4343-436, 474-478.

Coon, M.D., and Evans, R.J. (1971). "Recoverable Deformation of Cohesionless Soils", Journal of the Soil Mechanics and Foundation Division, ASCE, Vol. 97, SM2, pp. 375-391.

Cundall, P.A. and Strack, O.D.L. (1979). "A Discrete Numerical Model for Granular Assemblies". Geotechnique, Vol. 29, No. 1, pp. 47-65.

Davis, R.A. and Deresiewicz, H. (1977). "A Discrete Probabilistic Model for Mechanical Response of a Granular Medium". Acta Mechanica, 27, pp. 69-89.

Deresiewicz, H. (1958a), "Stress-Strain Relations for a Simple Model of a Granular Medium", Journal of Applied Mechanics, ASME, Sept., pp. 402-406.

Dobry R., Ladd, R.S., Yokel, F.Y., Chung, R.M., and Powell, D. (1982), "Prediction of Pore Water Pressure Buildup and Liquefaction of Sands during Earthquakes by the Cyclic Strain Method". Building Science Series 138, National Bureau of Standards.

Dobry, R., Ng, T., Petrakis, E. and Seridi, A. (1988), "An Incremental Elastic-Plastic Model for the Force-Displacement Relation at the Contact Between Elastic Spheres". Submitted for Publication, Journal of Engineering Mechanics, ASCE.

Drnevich, V.P. and Richart, F.E., Jr (1970), "Dynamic Prestraining of Dry Sand". Journal of the SMFD, ASCE, 96, SM2, March, pp. 453-469.

Duffy, J. and Mindlin, R.D. (1957), "Stress-Strain Relations and Vibrations of a Granular Medium", J. Appl. Mech., ASME, Dec., pp. 585-593.

Duffy, J. (1959), "A Differential Stress-Strain Relation for the Hexagonal Close-Packed Array of Elastic Spheres". J. Appl. Mech., 26, pp. 88-94.

Hardin, B.O, and Richart, F.E. (1963), "Elastic wave Velocities in Granular Soils", J. Soil Mech. Found. Div., ASCE, Vol. 89, SM1, pp. 33-65.

Hardin, B.O., and Black, W.L. (1966), "Sand Stiffness Under Various Triaxial Stresses". J. soil Mech. Found. Div., ASCE, Vol. 94, SM2, pp. 27-42.

Hertz, H. (1882), "Uber die Beruhrungsfester Elastische Korper". Journal Reine Angew. Mathematik, 92, pp. 156-171.

Knox, D.P., Stokoe, K.H., and Kopperman, S.E (1982), "Effect of State of Stress on Velocity of Low Amplitude Shear Waves Propagating Along Principal Stress Directions in Dry Sand". Geotechnical Engineering Report, GR82-23, University of Texas, Austin, TX.

Kopperman, S.E., Stokoe, K.H., and Knox, D.P. (1982), "Effect of State of Stress on Velocity of Low Amplitude Compression Waves Propagating Along Principal Stress Directions in Sand". Geotechnical Engineering Report, GR82-22, University of Texas, Austin, TX.

Lade, P.V., and Nelson, R.B. (1987), "Modelling the Elastic Behavior of Granular Materials". International Journal for Numerical and Analytical Methods in Geomechanics, Vol. 11, pp. 521-542.

Mindlin, R.D. (1949). "Compliance of Elastic Bodies in Contact". J. Applied Mech., ASME Sept., pp. 259-268.

Mindlin, R.D. and Deresiewicz, H. (1953), "Elastic Spheres in Contact under Varying Oblique Forces". J. Applied Mechanics, ASME, Sept., pp. 327-344.

Ng, T. and Dobry, R. (1988), "Computer Modeling of Granular Soils Under Cyclic Loading: A Particulate Mechanics

Approach". Report CE-88-03, Department of Civil Engineering, Rensselaer Polytechnic Institute, Troy, NY.

Oda, M. (1974), "A Mechanical and Statistical Model of Granular Material". Soils and Foundations, Vol. 14, No. 1, pp. 13-27.

Oda, M., Konishi, J. (1974), "Microscopic Deformation Mechanism of Granular Material in Simple Shear". Soils and Foundations, Vol. 14, No. 4, pp. 25-38.

Oda, M., Konishi, J. and Nemat-Nasser, S., (1983), "Experimental Micromechanical Evaluation of the Strength of Granular Materials; Effects of Particle Rolling". Mechanics of Granular Materials: Models and Constitutive Relations, Jenkins and Satake, eds. , pp. 21-30.

Oda, M., Nemat-Nasser S., and Konishi, J., (1985), "Stress Induced Anisotropy in Granular Masses". Soils and Foundations, Vol. 25, No. 3, pp. 85-97.

Petrakis, E. and R. Dobry (1986), "A Self Consistent Estimate of the Elastic Constants of a Random Array of Equal Spheres with Application to Granular Soil under Isotropic Conditions", Report CE-86-04, Rensselaer Polytechnic Institute, Troy, NY.

Petrakis, E. and Dobry, R. (1987), "A Two-Dimensional Numerical Micromechanical Model for a Granular Soil at Small Strains", Report CE-87-01, Rensselaer Polytechnic Institute, Troy, NY.

Petrakis, E. and Dobry, R. (1988a), "Small-Strain Elastic Constants of Precycled Sand by the Self-Consistent Method". Submitted for publication, Journal of Engineering Mechanics, ASCE.

Petrakis, E. and Dobry, R. (1988b), " A Two-Dimensional Numerical Micromechanical Model for a Granular Cohesionless Material at Small Strains". Proceedings, American Physical Society, New Orleans, LA.

Poritsky, H. (1950), " Stresses and deflections of Cylindrical Bodies in Contact with Application to Contact of Gears

and of Locomotive Wheels". J. Appl. Mechanics, ASME, June, pp. 191-201.

Roesler, S.K. (1979), "Anisotropic Shear Modulus due to Stress Anisotropy". J. Geotech. Engr. Div., ASCE, Vol. 105, GT5, pp. 871-880.

Rowe, P.W. (1971), "Theoretical Meaning and Observed Values of Deformation Parameters for Soil", Proc. Roscoe Memorial Symposium Stress-Strain Behavior of Soils, pp. 143-194.

Schmertmann, J.H. (1978), "Effect of Shear Stress on Dynamic Bulk Modulus of Sand". Technical Report S-78-16, October, US Army Waterways Experiment Station, Vicksburg, MS.

Seed, H.B., and Idriss, I.M. (1970), "Soil Moduli and Damping Factors for Dynamic Response Analyses". Report UCB/EERC-70/10, University of California, Berkeley, CA.

Seed, H.B., Wong, R.T., Idriss, I.M., and Tokimatsu, K. (1984), "Moduli and Damping Factors for Dynamic Analyses of Cohesionless Soils", Report UCB/EERC-84/14, University of California, Berkeley, CA.

Seridi, A., and Dobry, R. (1984), "An Incremental Elastic-Plastic Model for the Force-Displacement Relation at the Contact Between Two Spheres". Report CE-84-06, Department of Civil Engineering, Rensselaer Polytechnic Istitute, Troy, NY.

Serrano, A.A. and Rodriguez-Ortiz, J.M., "A Contribution to the Mechanics of Heterogeneous Granular Media". Symp. Plast. and Soil Mechanics, Cambridge, U.K.

Shahinpoor, M. and Shahrpass, A. (1982), "Frequency Distribution of Voids in Monolayers and Randomly Packed Equal Spheres". Bulk Solids Handling, Vol. 2, 4, pp. 825-838.

Smith, W.O., Foote, P.D., and Busang, P.F. (1929), "Packing of Homogeneous Spheres", Phys. Review, 34, pp. 1271-1274.

Sokolnikoff, I.S. (1956), Mathematical Theory of Elasticity, McGraw Hill, New York, NY.

Stokoe, K.H., Roesset, J.M., Knox, D.P., Kopperman, S.E. and Sudhiprakarn, C. (1980), "Development of a Large-Scale Triaxial Testing Device for Wave Propagation Studies". Geotechnical Report GR80-10, University of Texas, Austin, TX.

Strack, O.D.L. and Cundall, P.A. (1984), "Fundamental Studies of Fabric in Granular Materials, Report, Department of Civil and Mineral Engineering, University of Minnesota, Mineapolis, MN.

Vaid, Y. P., and Chern, J.C., (1983), "Effects of Static Shear on Resistance to Liquefaction". Soils and Foundations, Vol. 23, No. 1, pp. 47-60.

Walton, K, (1987), "the Effective Elastic Moduli of a Random Packing of Spheres". J. Mech. Phys. Solids, Vol. 26, pp. 139-150.

White, J.E. (1965). Seismic Waves, McGraw Hill, New York, NY.

Yanagisawa, E. (1983), "Relation Between the Dynamic Shear Modulus and Void ratio in Granular Media". Advances in the Mechanics and Flow of Granular Materials, Vol. II, M. Shahinpoor, ed., Trans Tech Publications, Claustahl-Zellerfeld, Fed. Rep. Germany.

Yu, P. and Richart, F.E. (1984), "Stress Ratio Effects on Shear Modulus of Dry Sands". J. of the Geotec. Engr. Div., ASCE, Vol. 110, GT3, pp. 331-345.

Zhang, Y., and Cundall, P.A. (1986), "Numerical Simulation of Slow Deformations". Proceedings, Tenth U.S. National Congress of Applied Mechanics, University of Texas, Austin, TX.

TABLE 1

(after Ng and Dobry, 1988)

RPI COMPUTER PROGRAM

CONBAL-2 = CONTact truBAL in 2d

TRUBAL (Peter Cundall)

- Distinct Element Method (Finite Difference)
- 3D Random Array of Spheres
- Periodic Space
- Linear, Pressure-Independent, Arbitrary Contact Compliance

CONTACT (RPI)

- General Solution Mindlin-Hertz Contact Problem for Two Identical Spheres
- Reproduces Identically all Available Analytical Results
- Program Accepts as Input Aribitrary Time History of Force or Displacement
- Can be Used Approximately for Case of Two Spheres of Somewhat Different Sizes

CONBAL-2 = TRUBAL + CONTACT - 1D + VECTORIZATION

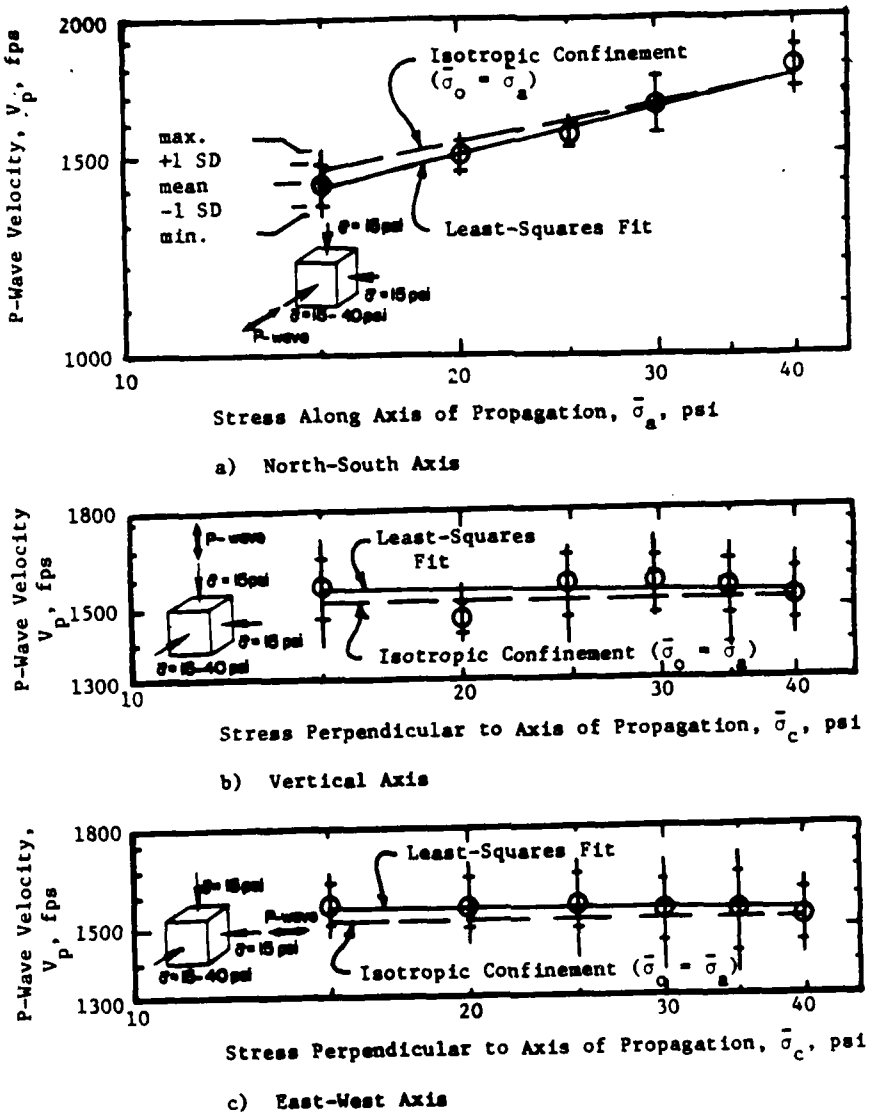

Figure 1. Effect of Structural Anisotropy on Compression Wave Velocity for Triaxial Confinement (after Kopperman et al, 1982).

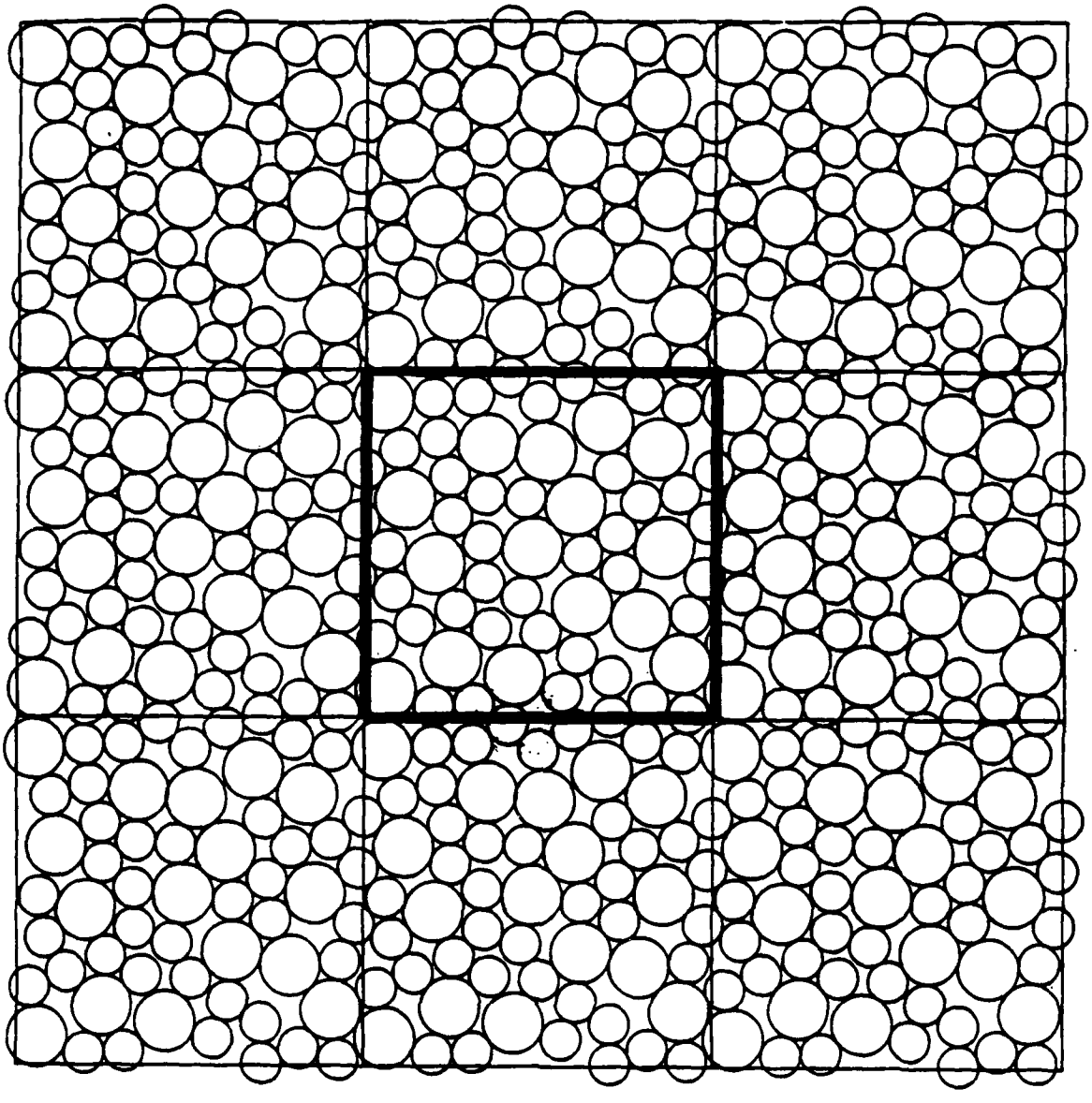

Figure 2. Random Array of Spheres Generated by Program TRUBAL

DISTINCT ELEMENT METHOD

(Programs BALL, TRUBAL developed by Peter Cundall)

Time t

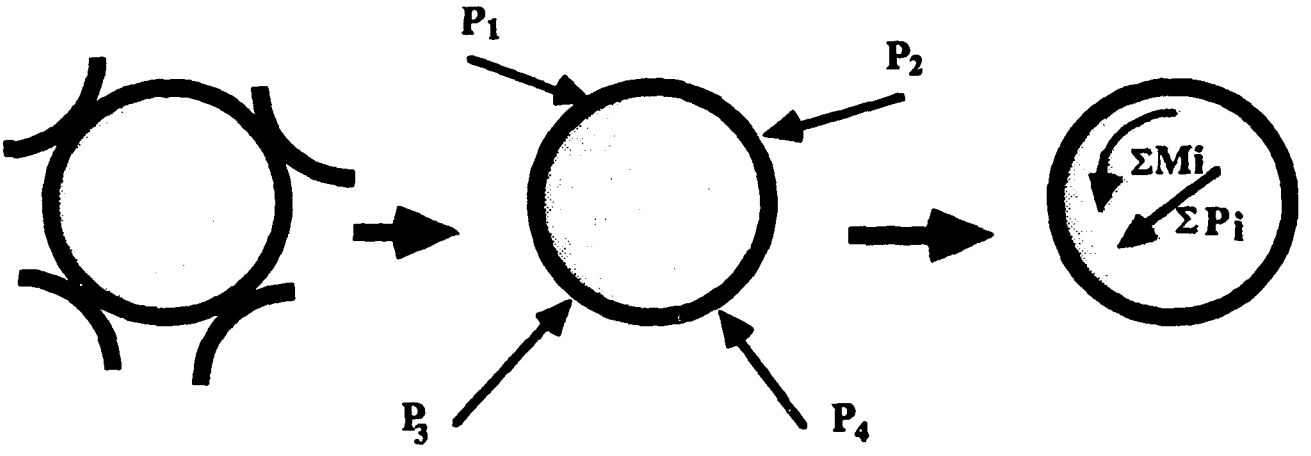

ΣPi produces acceleration of particle
ΣMi produces angular acceleration (spin) of particle

Acceleration and Spin Computed as if Neighboring Particles did not exist. Time step is assumed to be small such that accelerations and velocities are constant in this small time.

Time t + Δt

- **Particle occupies new position due to acceleration**
- **New Pi's, Mi's are computed for new positions**
- **ΣPi, ΣMi and process is repeated.**

Figure 3. Outline of the Main Features of the Distinct Element Method

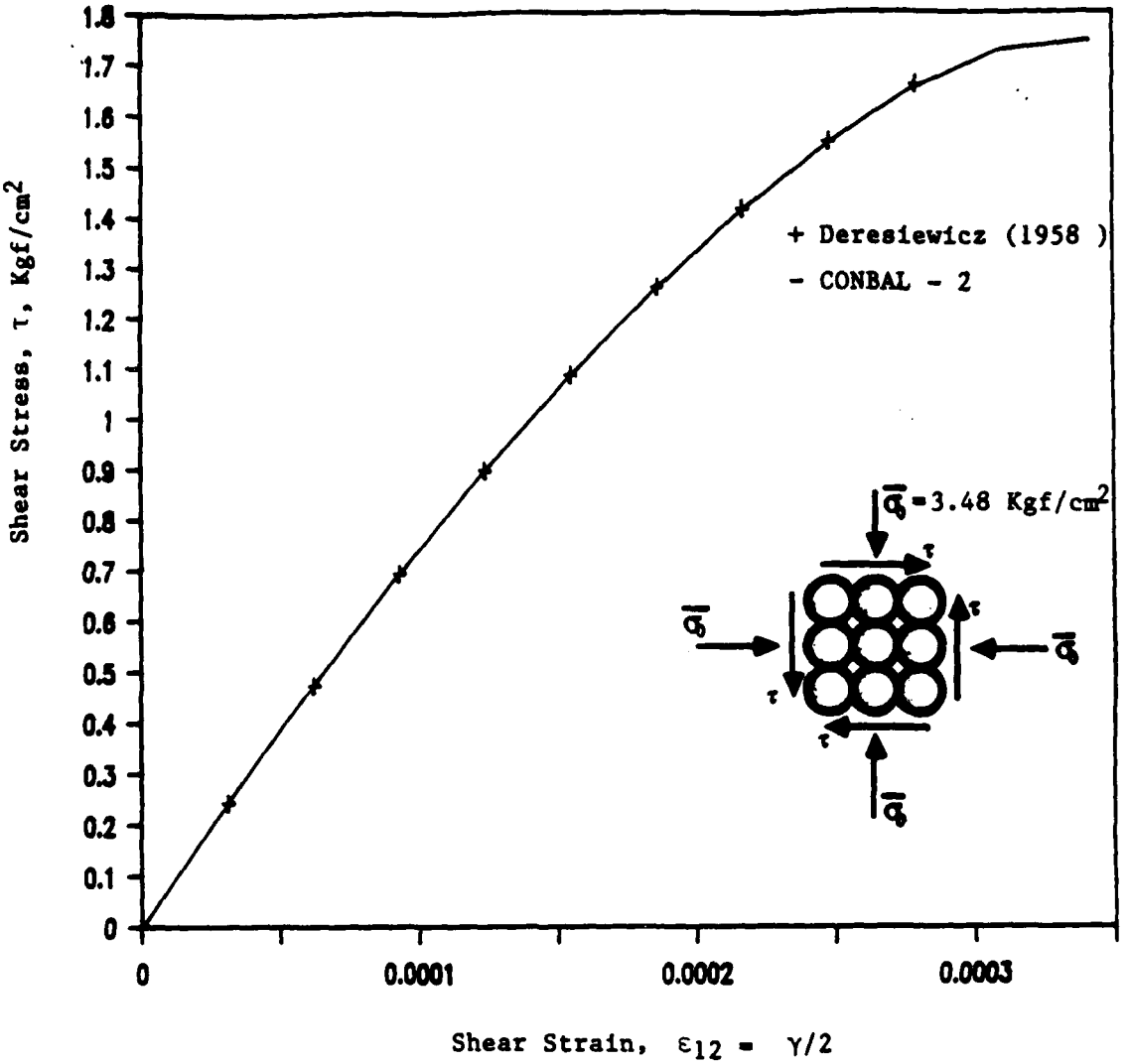

Figure 4. Simple Cubic Array in 2-D Subjected to Pure Shear: Comparison Between Analytical and Numerical (CONBAL-2) results. (after Ng and Dobry, 1988)

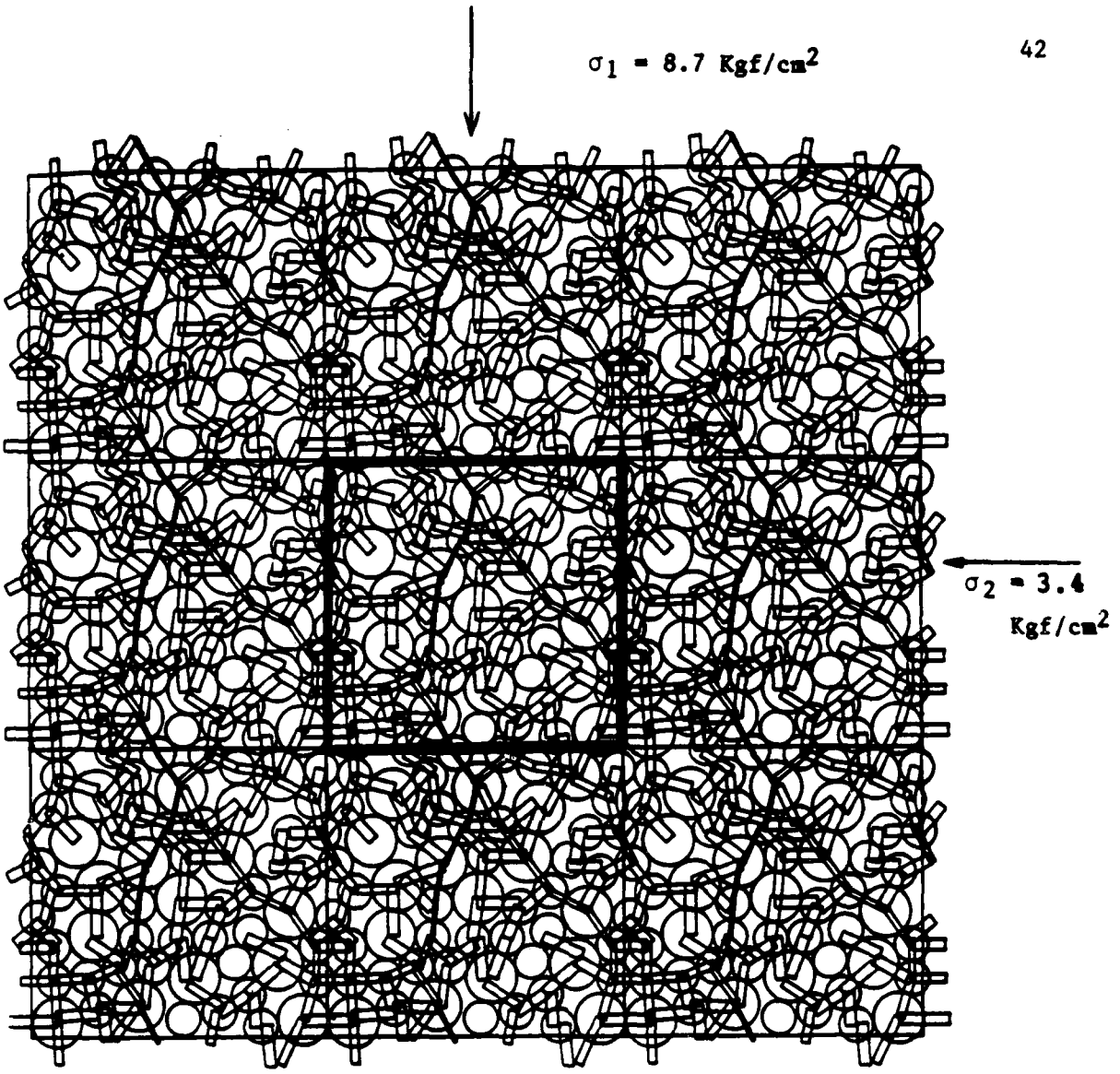

Figure 5. A Random, Periodic, 2-D Medium of 57 Elastic, Rough, Quartz, Spheres, of two Radii (R_1/R_2=1.5), Subjected to Biaxial Compression. Note the "window" with the representative random pattern (after Ng and Dobry, 1988)

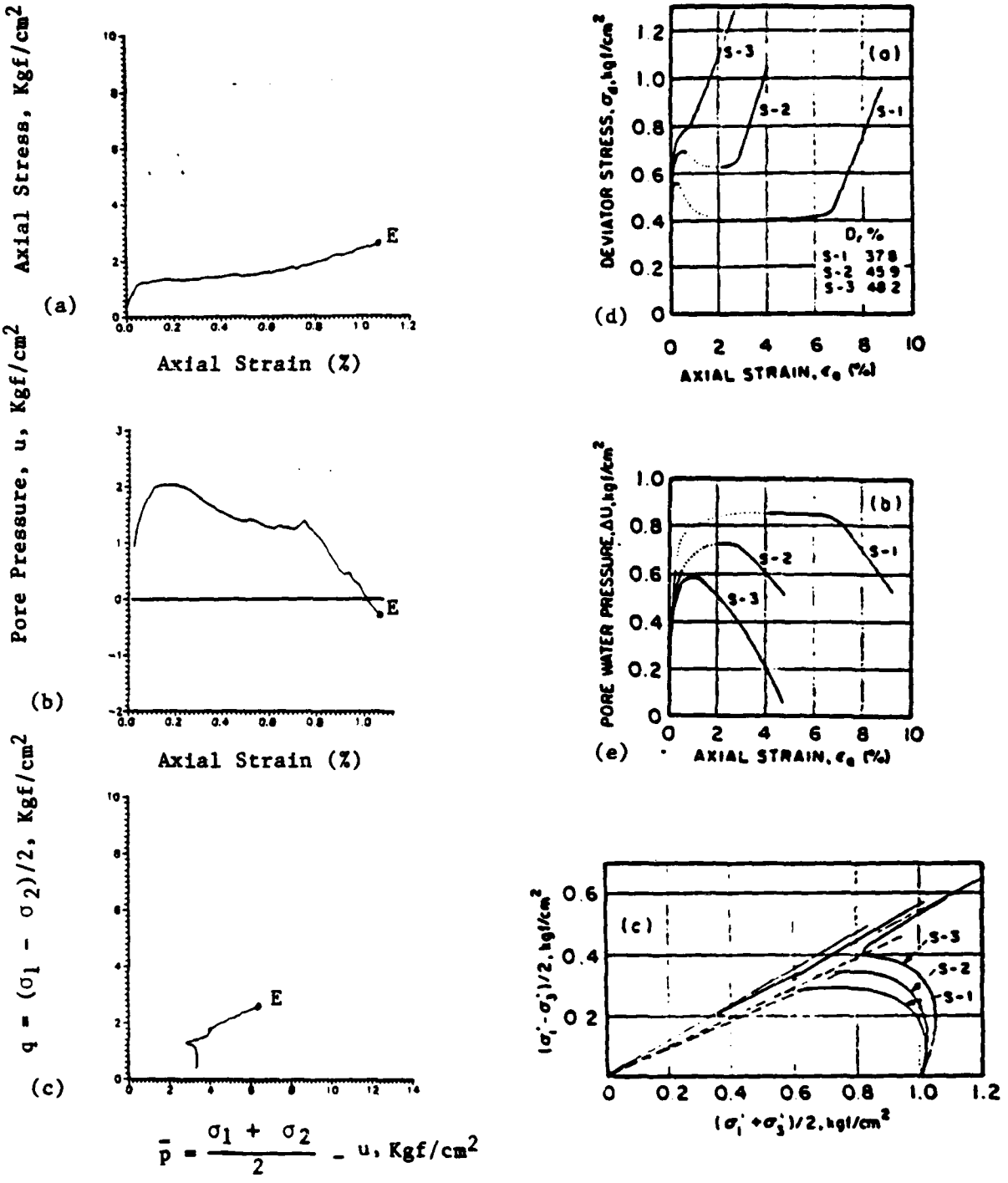

Figure 6. Stress-Strain Response of the Random Two-Dimensional Array of Figure 5 subjected to biaxial compression (a, b, c) and Stress-Strain Response of Medium Dense sand Under Monotonic Compressive Loading (after Vaid and Chern, 1983 - d, e, f, Test S-3;)
Note: Figure reproduced after Ng and Dobry (1988).

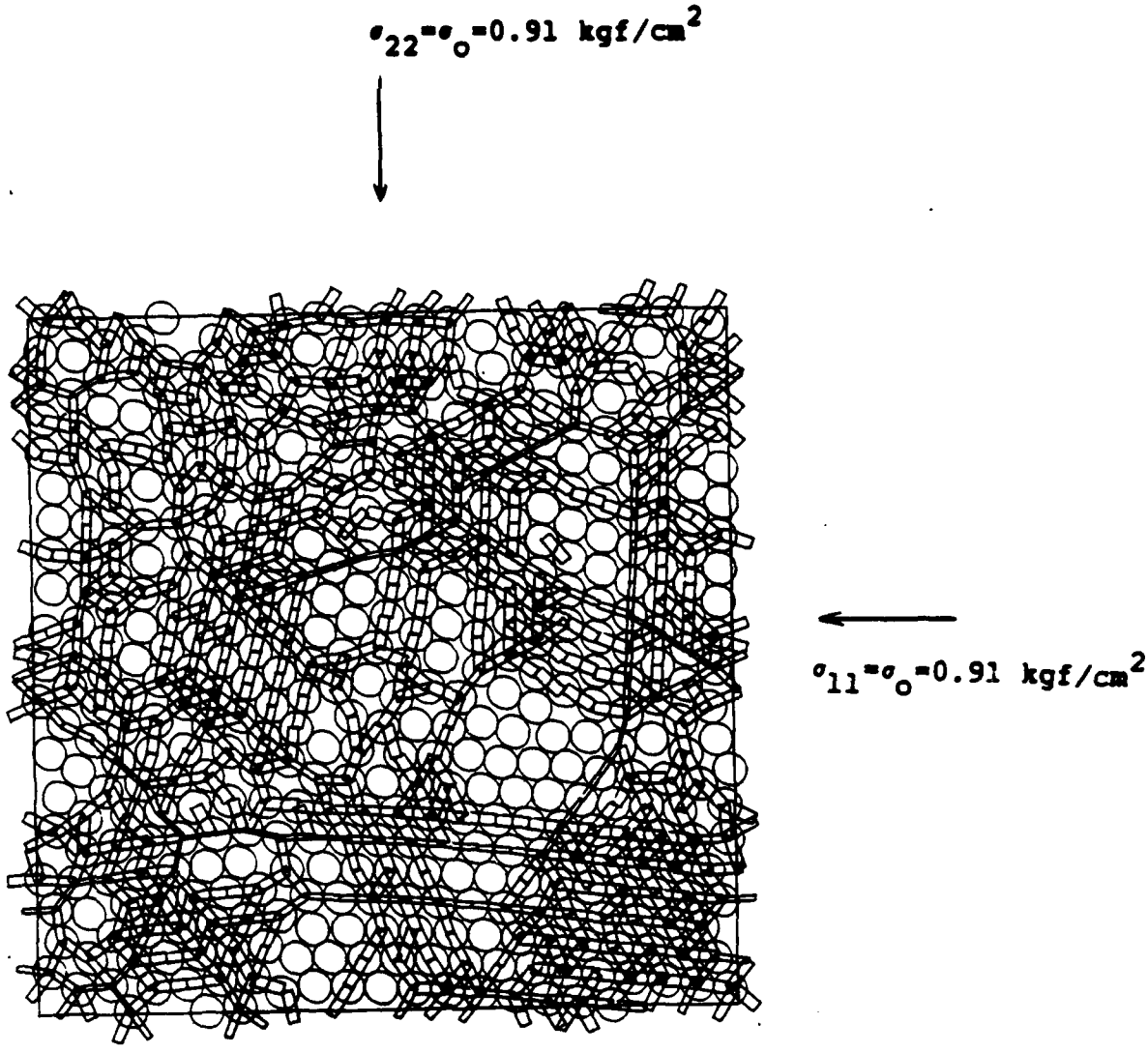

Figure 7. 2-D Random Array of 477 Equal, Elastic, Rough, Quartz Spheres Subjected to Isotropic Compression, $\sigma_o=0.91$ kgf/cm^2. Note that this figure represents the "window" with the representative random pattern.

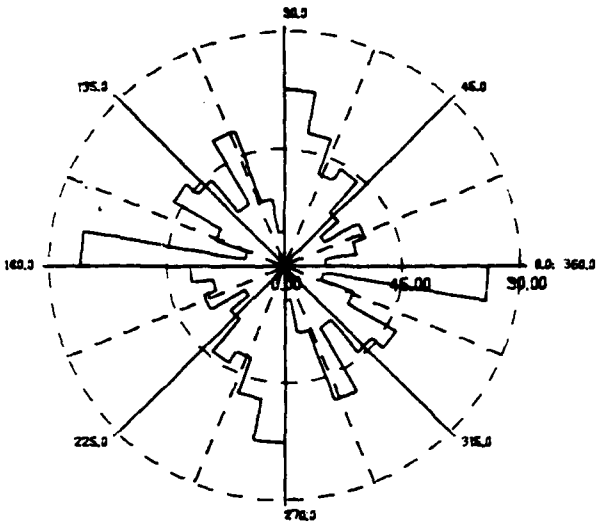

FREQUENCY DISTRIBUTION
OF CONTACT ANGLE

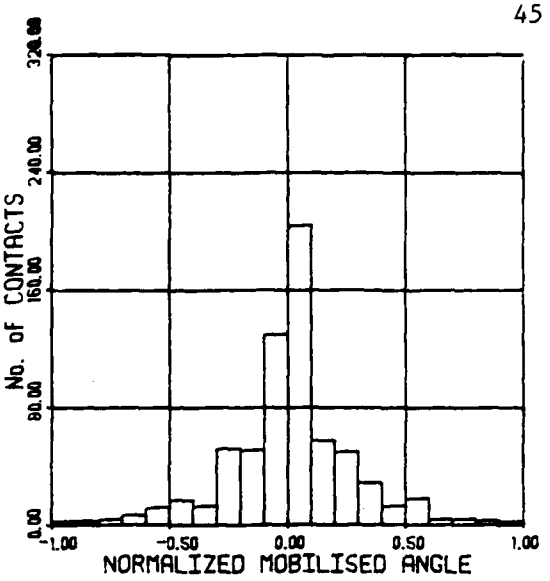

FREQUENCY DISTRIBUTION
OF MOBILISED ANGLE

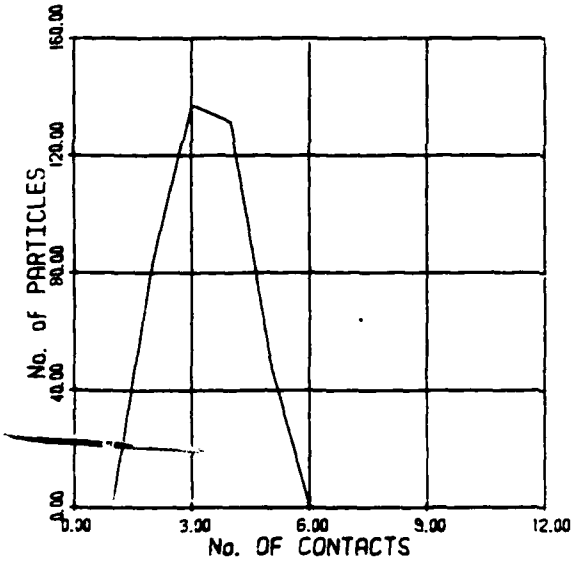

FREQUENCY DISTRIBUTION
OF CONTACT PER PARTICLE

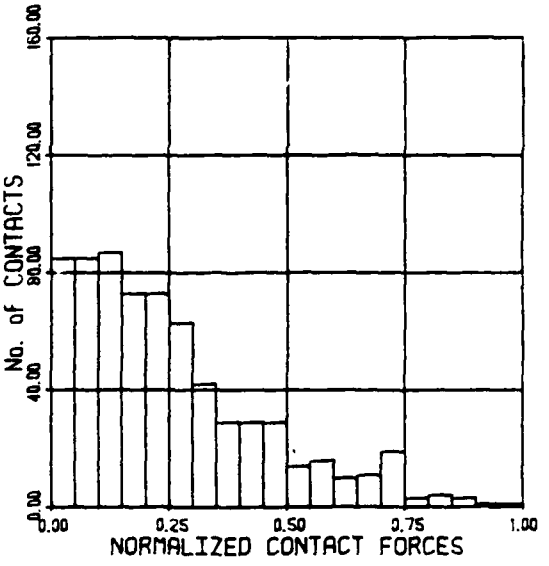

FREQUENCY DISTRIBUTION
OF CONTACT FORCE

Figure 8. Statistical Information Regarding the Isotropic Compression at σ_o=0.91 kgf/cm^2 of the 477-sphere medium of Figure 7.

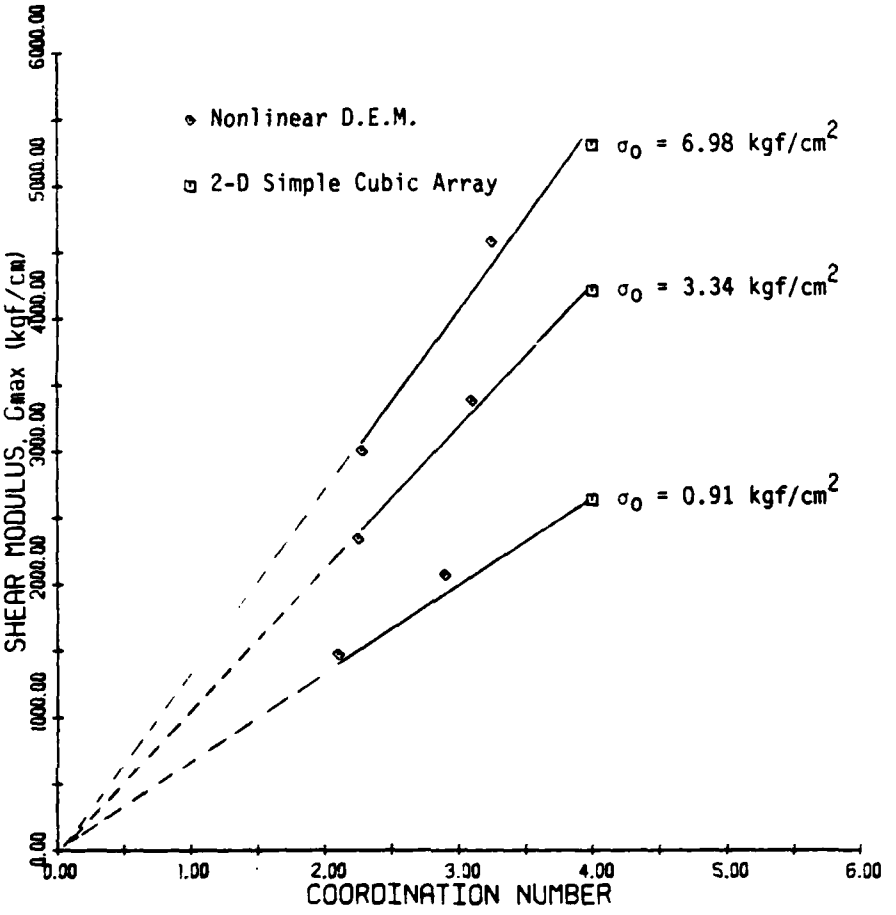

Figure 9. Shear Modulus, G_{max}, Versus Coordination Number (CN = Number of Contacts per Sphere) for two Random Arrays of 477 Equal, Quartz Spheres, and the Simple Cubic Array (CN=4).

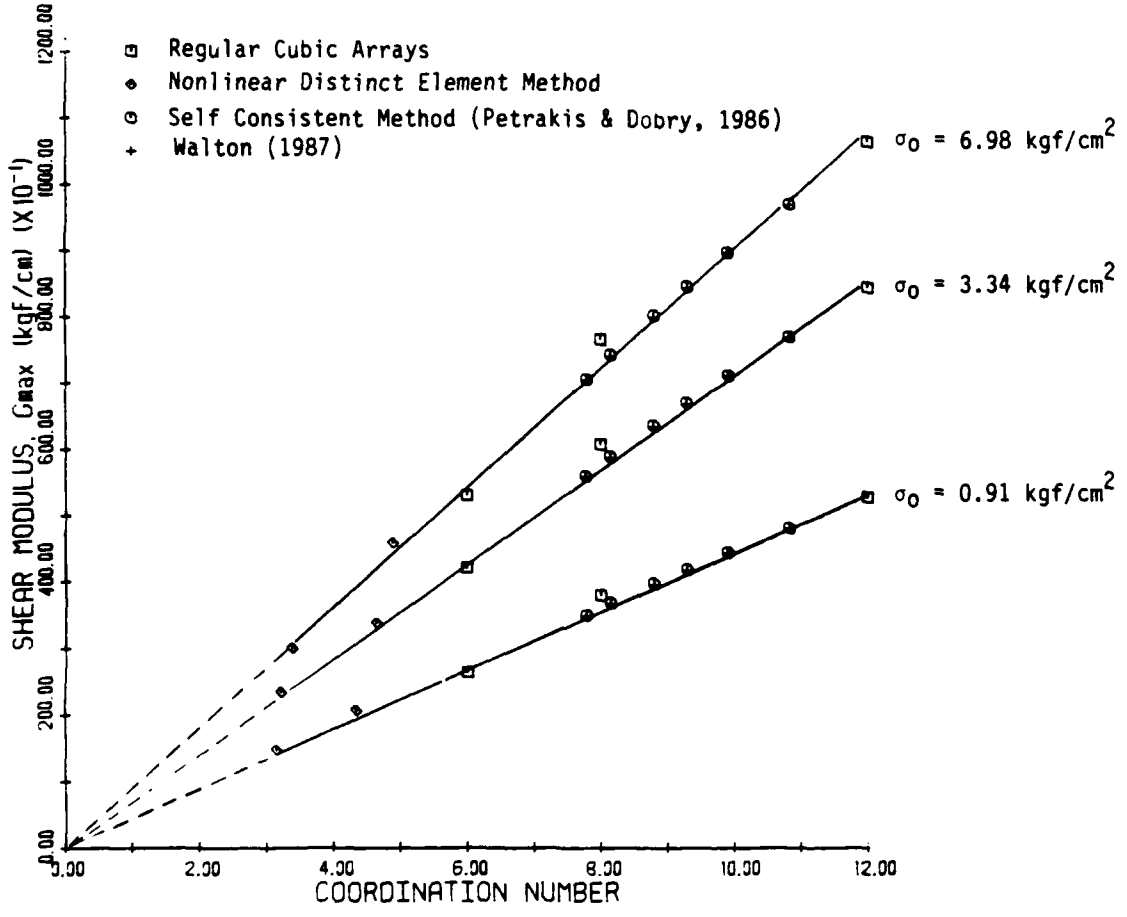

Figure 10. Shear Modulus, G_{max}, Versus Coordination Number for: i) two Random Arrays of 477 Equal Spheres, ii) Regular Arrays, and iii) Random Arrays of a given Porosity by the Self Consistent Method (Petrakis and Dobry, 1986) and the Analytical Expressions of Walton (1987). All spheres have been assigned the properties of quartz.

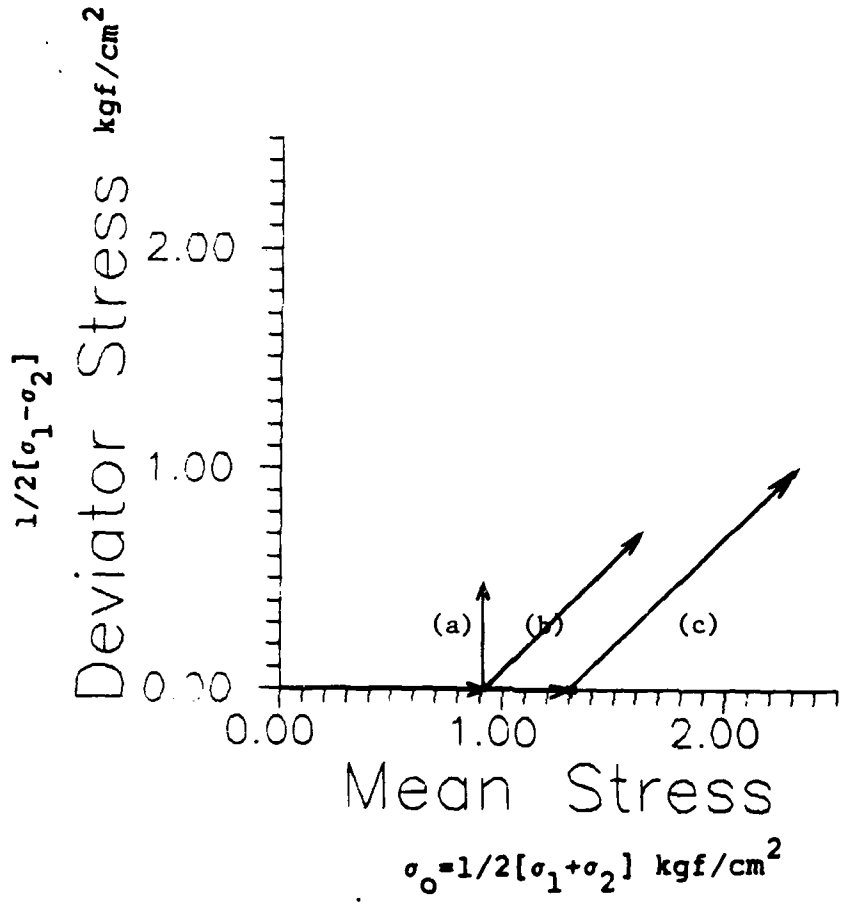

Figure 11. Stress Paths Used in the Simulations: (a)Biaxial Compression-Extension with Constant Mean Stress, σ_o=0.91 kgf/cm^2; (b)Biaxial Compression from σ_o=0.91 kgf/cm^2; and (c)Biaxial Compression, from σ_o=1.31 kgf/cm^2.

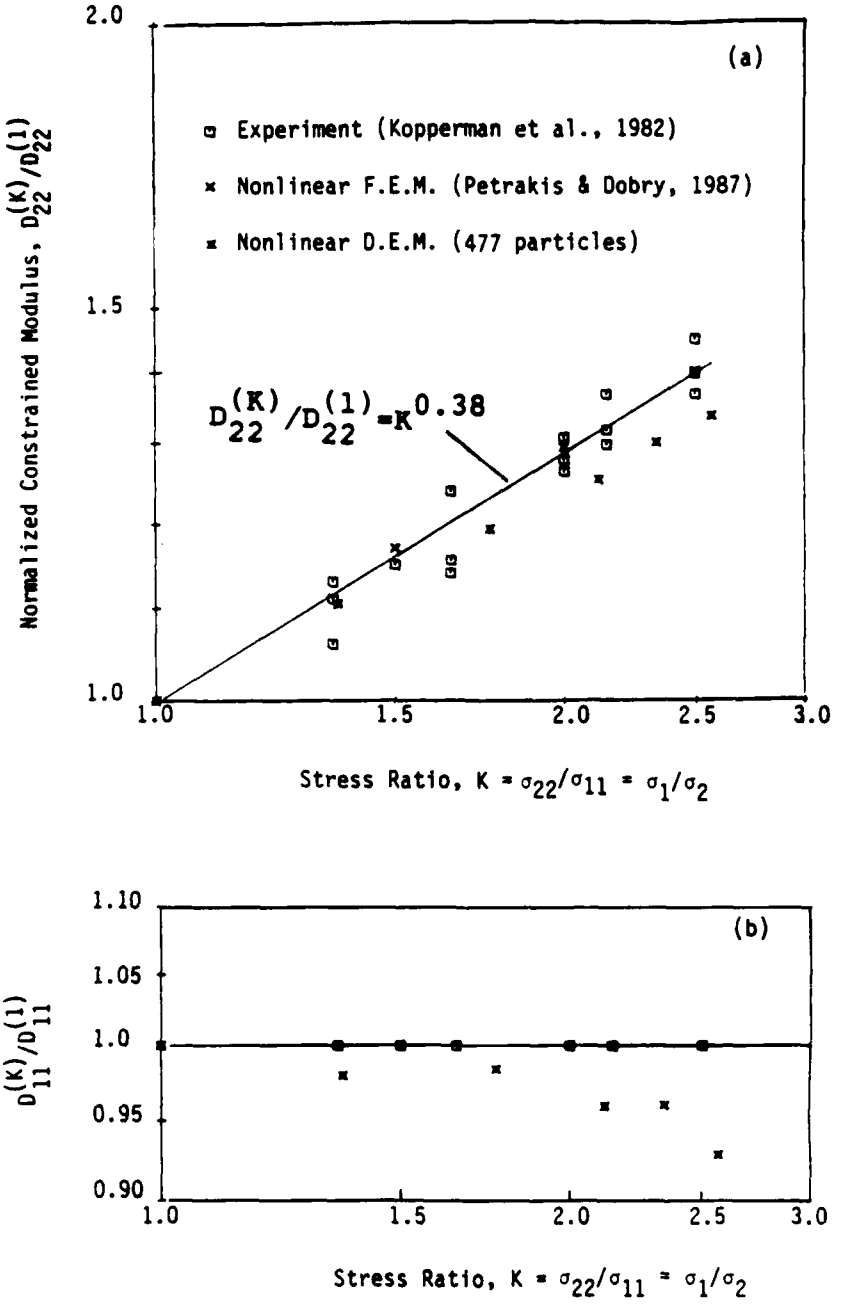

Figure 1. Normalized Constrained Moduli, $D_{ii}^{(K)}/D_{ii}^{(1)}$, Versus Stress Ratio, $K=\sigma_1/\sigma_2 = \sigma_{22}/\sigma_{11}$. Comparison Between Distinct Elewment, Finite Element and experimental Results: (a) In the Direction of σ_{22}, and (b)in the Direction of σ_{11} (σ_{11} is kept constant).

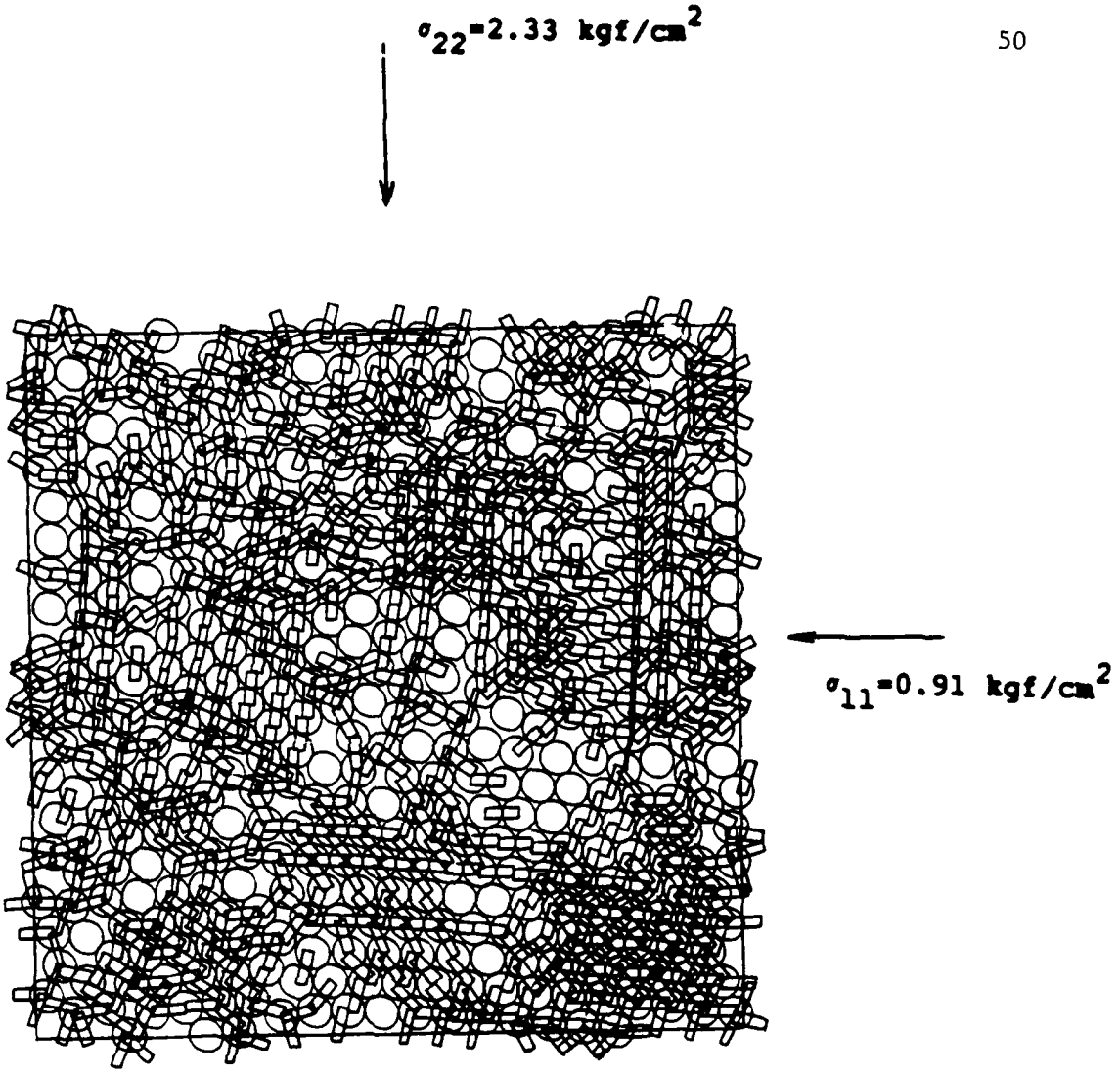

Figure 13. 2-D Random, Array of 477 Equal, Elastic, Quartz, Spheres Subjected to Biaxial Compression.

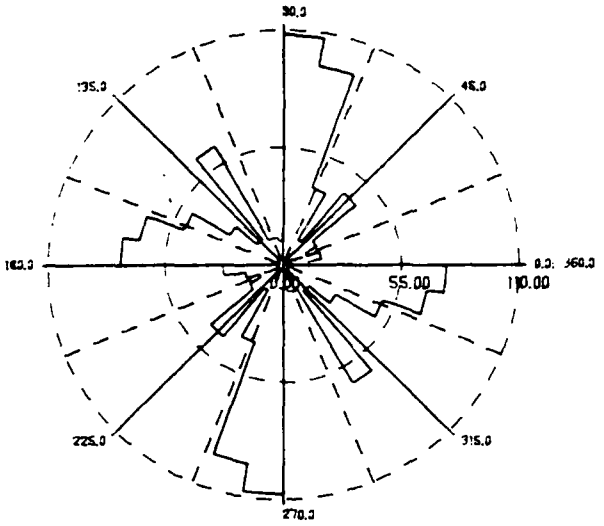

FREQUENCY DISTRIBUTION
OF CONTACT ANGLE

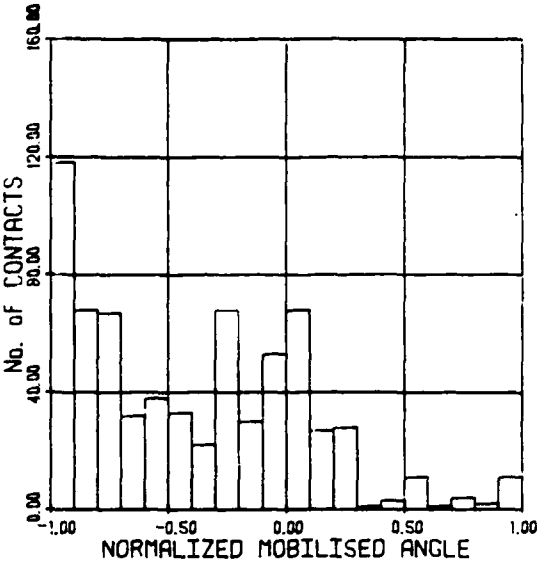

FREQUENCY DISTRIBUTION
OF MOBILISED ANGLE

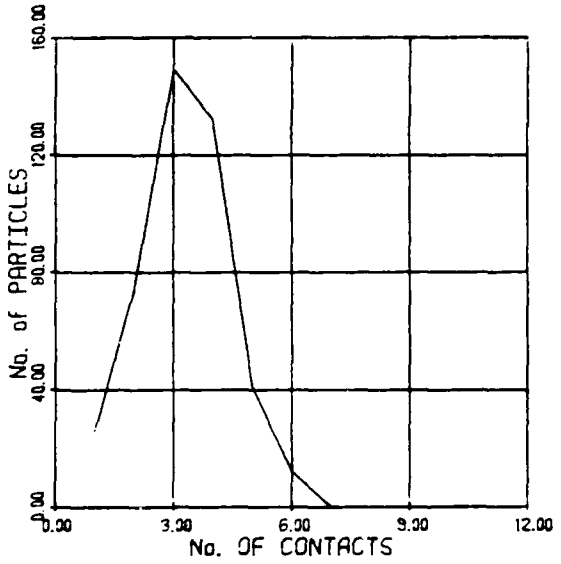

FREQUENCY DISTRIBUTION
OF CONTACT PER PARTICLE

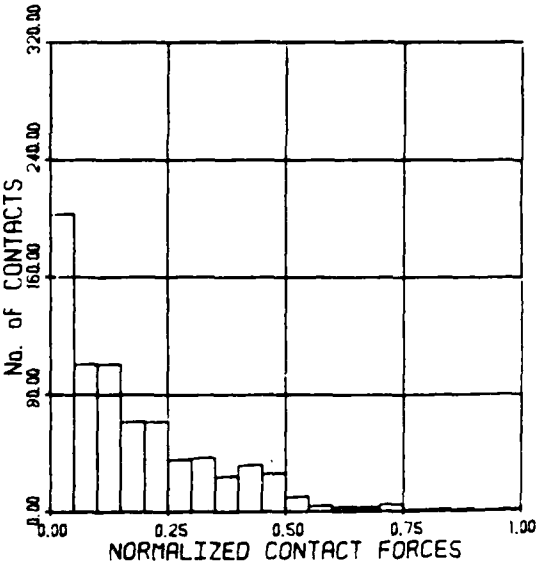

FREQUENCY DISTRIBUTION
OF CONTACT FORCE

Figure 14. Statistical Information Regarding the Biaxial Loading in Figure 13.

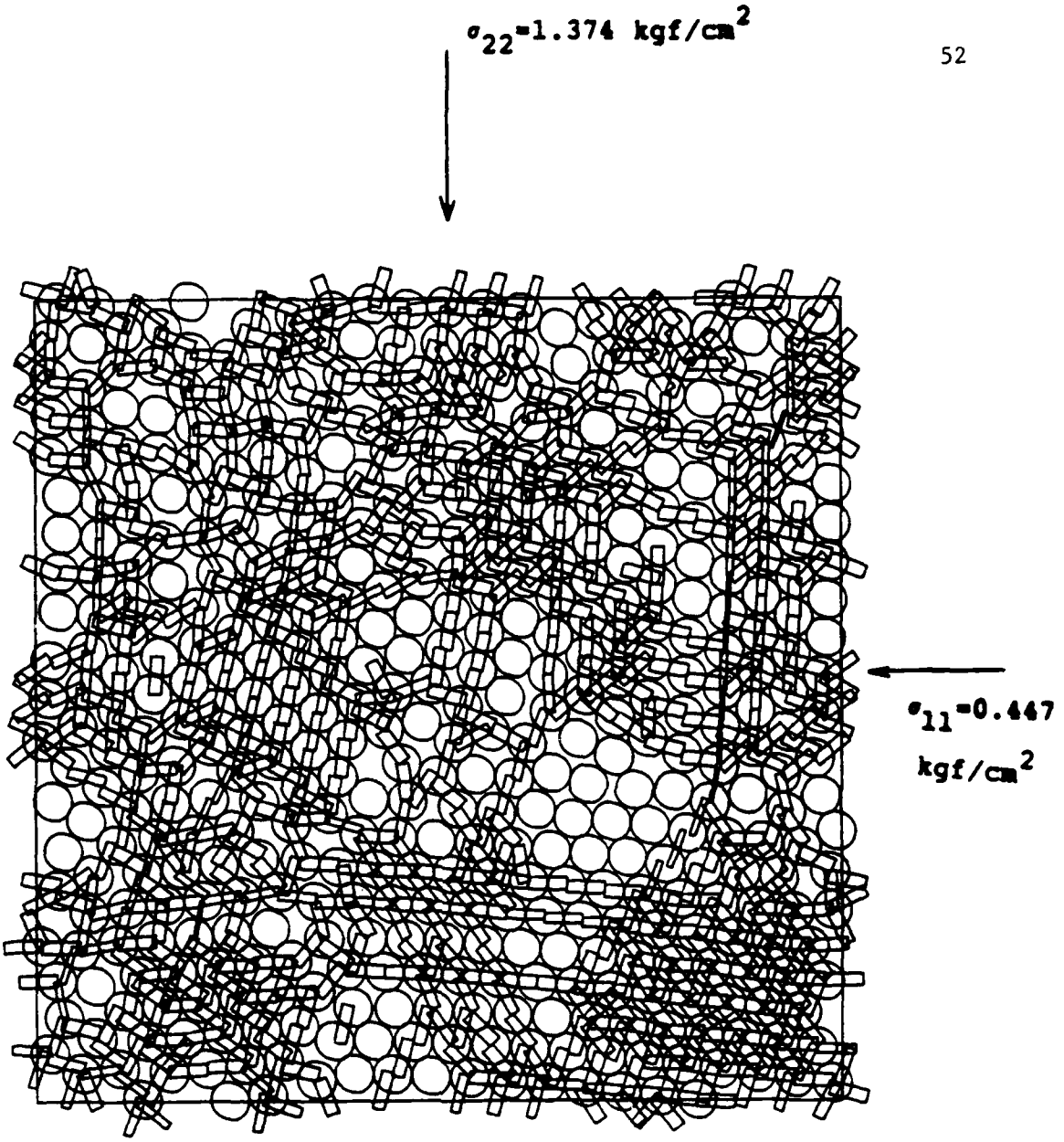

Figure 15. 2-D Random Array of 477 Equal, Elastic, Quartz Spheres Subjected to Biaxial Compression Extension with Constant Mean Stress σ_o= 0.91 kgf/cm^2.

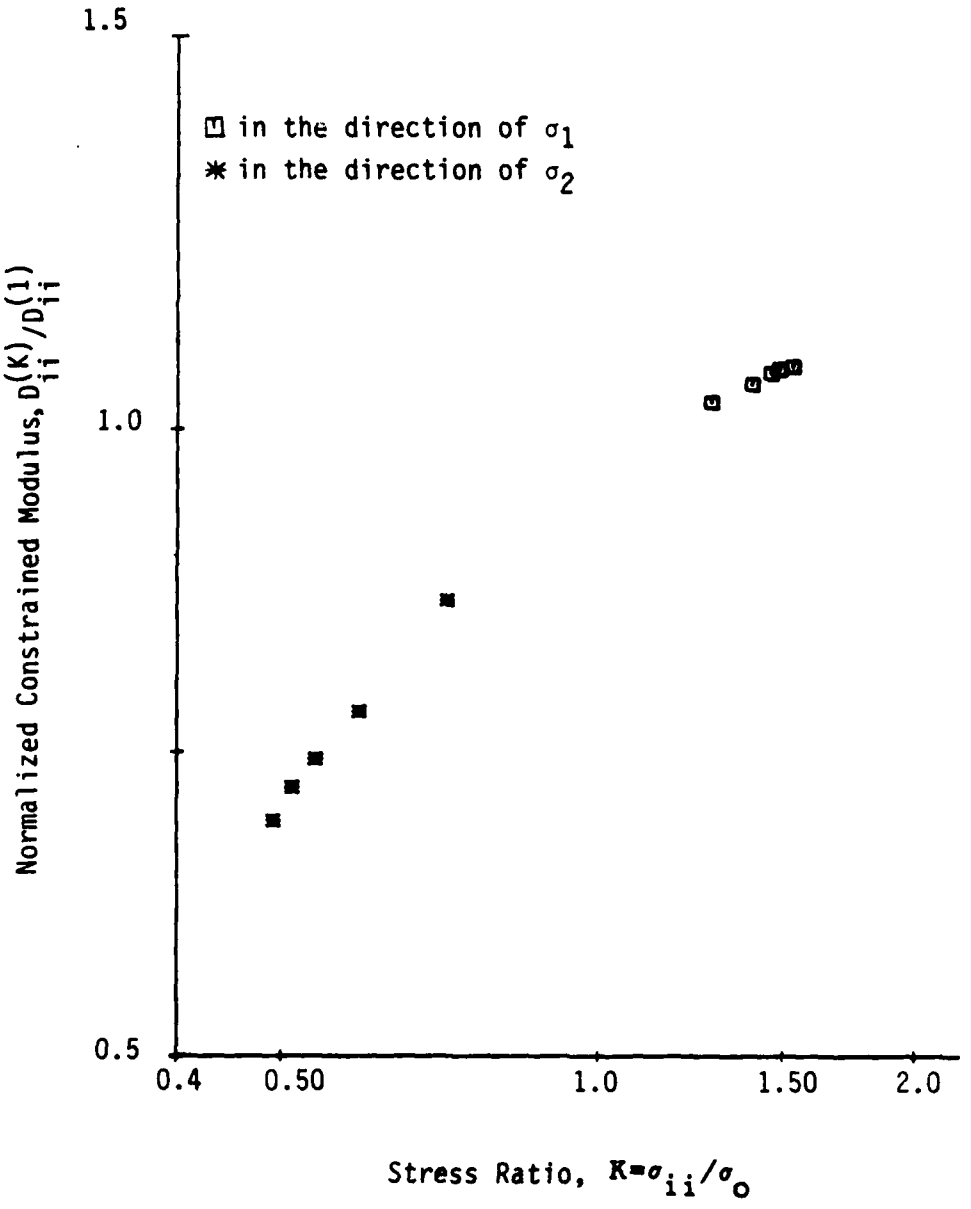

Figure 16. Normalized Constrained Moduli, $D_{ii}^{(K)}/D_{ii}^{(1)}$, Versus the Stress Ratio, $K=\sigma_{ii}/\sigma_o$, for the Case of Biaxial Compression-Extension Loading with Constant Mean Stress, σ_o=0.91 kgf/cm^2

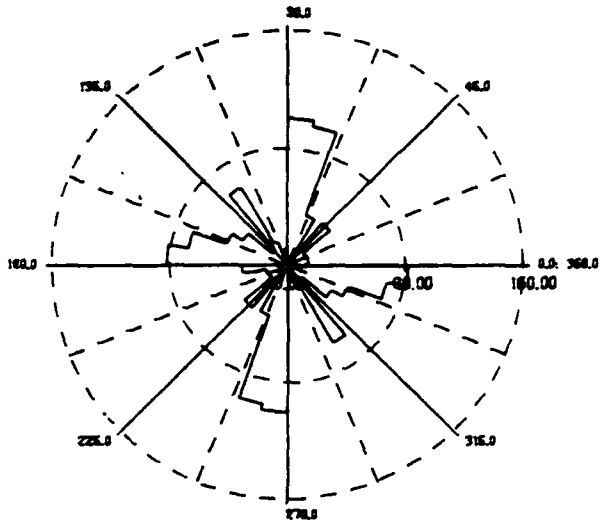

FREQUENCY DISTRIBUTION
OF CONTACT ANGLE

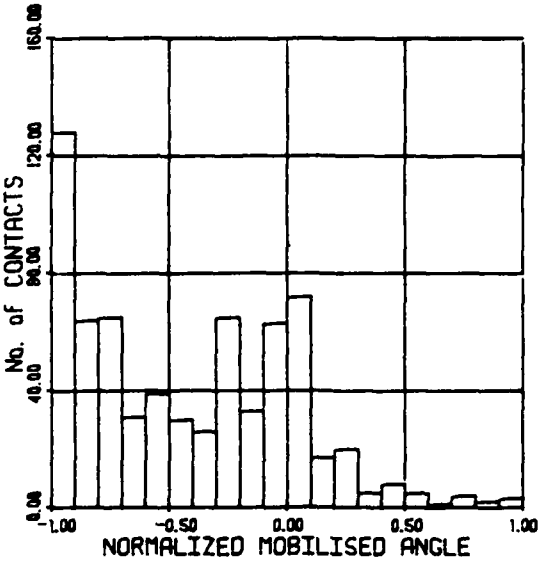

FREQUENCY DISTRIBUTION
OF MOBILISED ANGLE

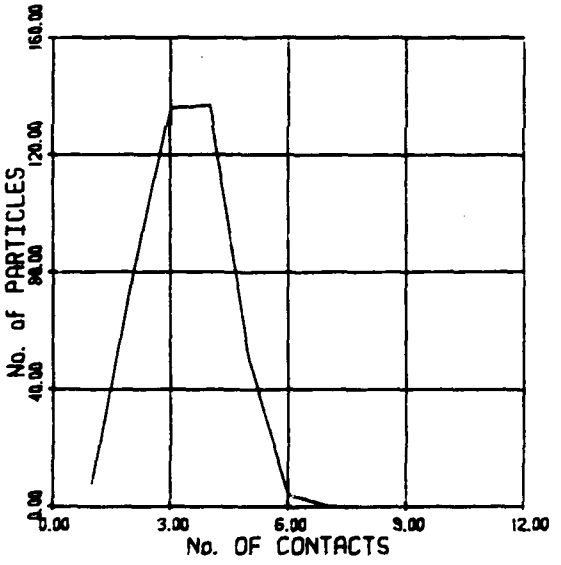

FREQUENCY DISTRIBUTION
OF CONTACT PER PARTICLE

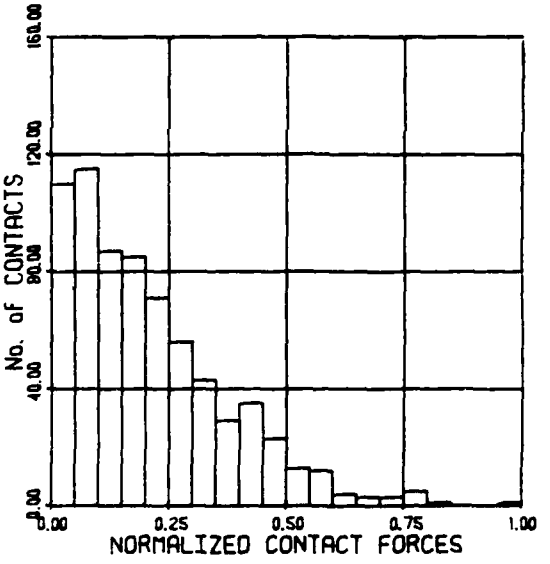

FREQUENCY DISTRIBUTION
OF CONTACT FORCE

Figure 17. Statistical Information for the of Biaxial Compression-Extension Loading in Figure 15.

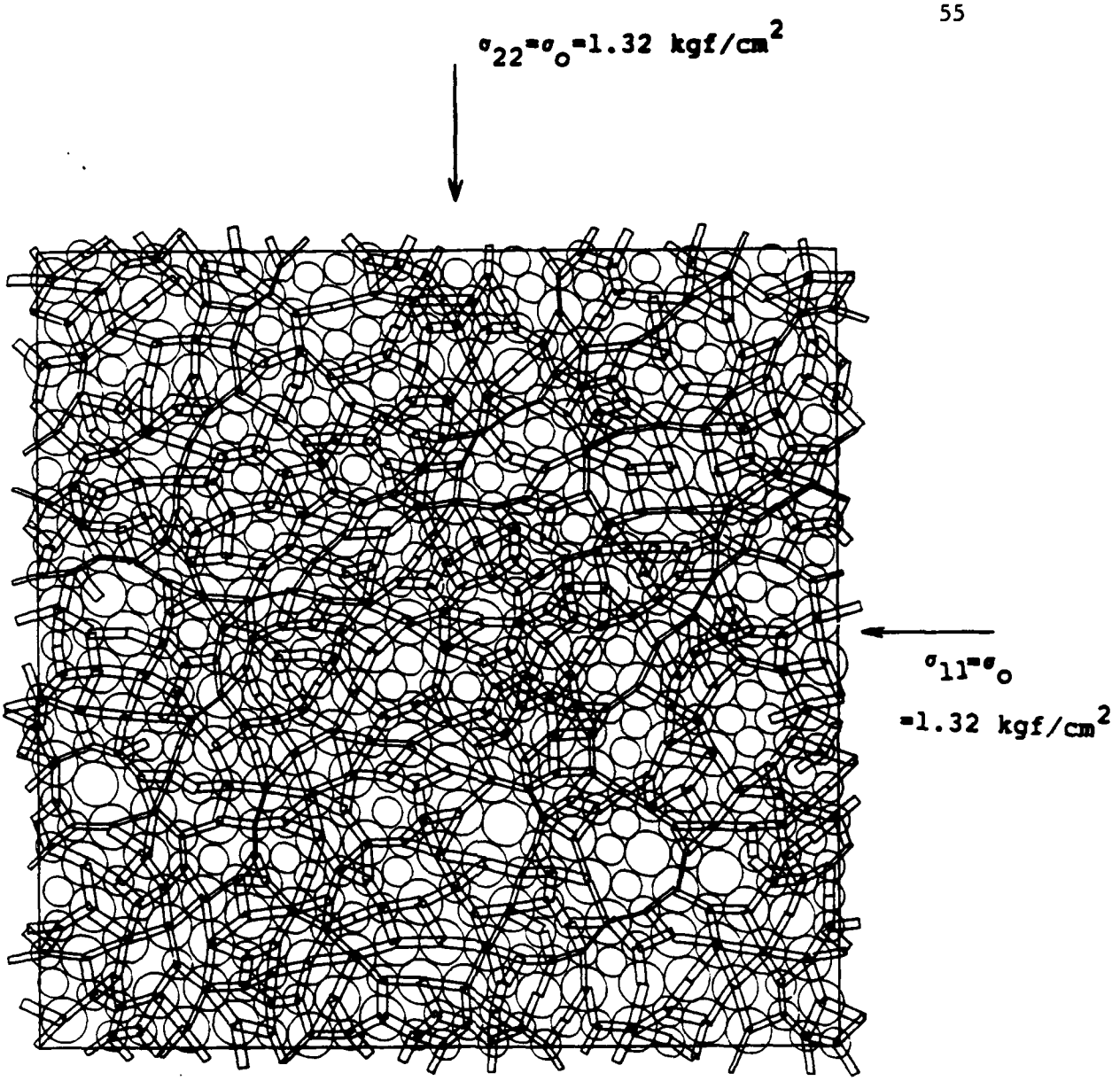

Figure 18. 2-D Random Array of 531 Elastic, Quartz Spheres of Two Radii ($R_1/R_2=1.5$) Subjected to Isotropic Compression $\sigma_o = 1.32$ kgf/cm^2

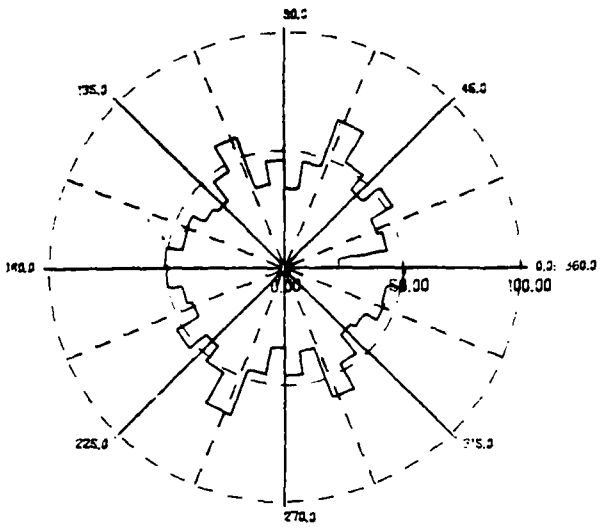

FREQUENCY DISTRIBUTION
OF CONTACT ANGLE

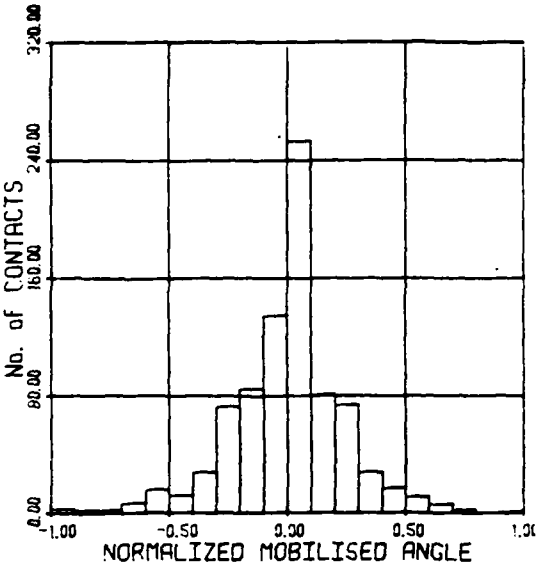

FREQUENCY DISTRIBUTION
OF MOBILISED ANGLE

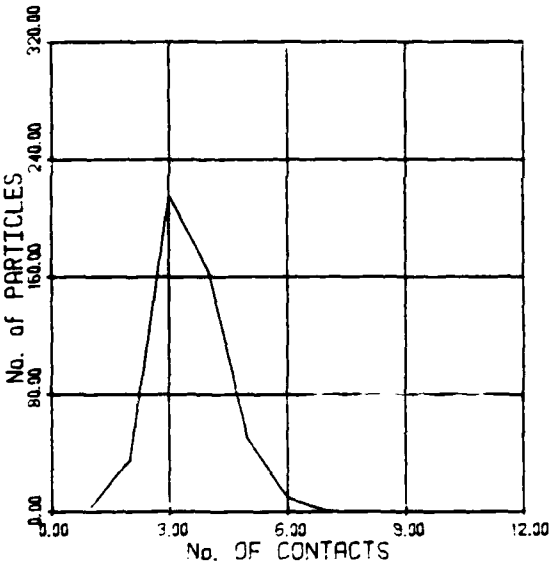

FREQUENCY DISTRIBUTION
OF CONTACT PER PARTICLE

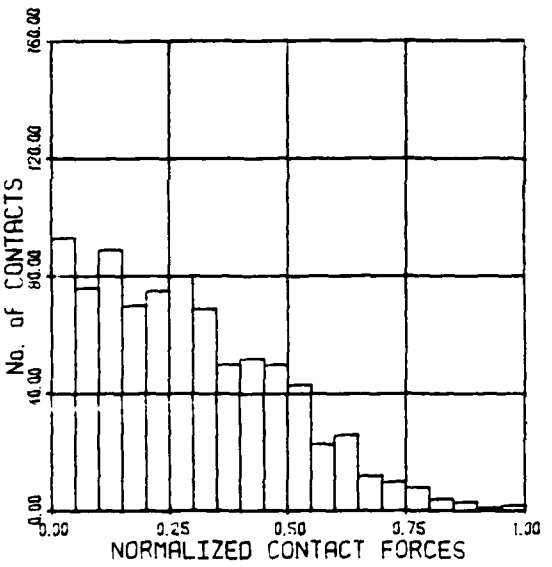

FREQUENCY DISTRIBUTION
OF CONTACT FORCE

Figure 19. Statistical Information for the Isotropic Compression Loading in Figure 18.

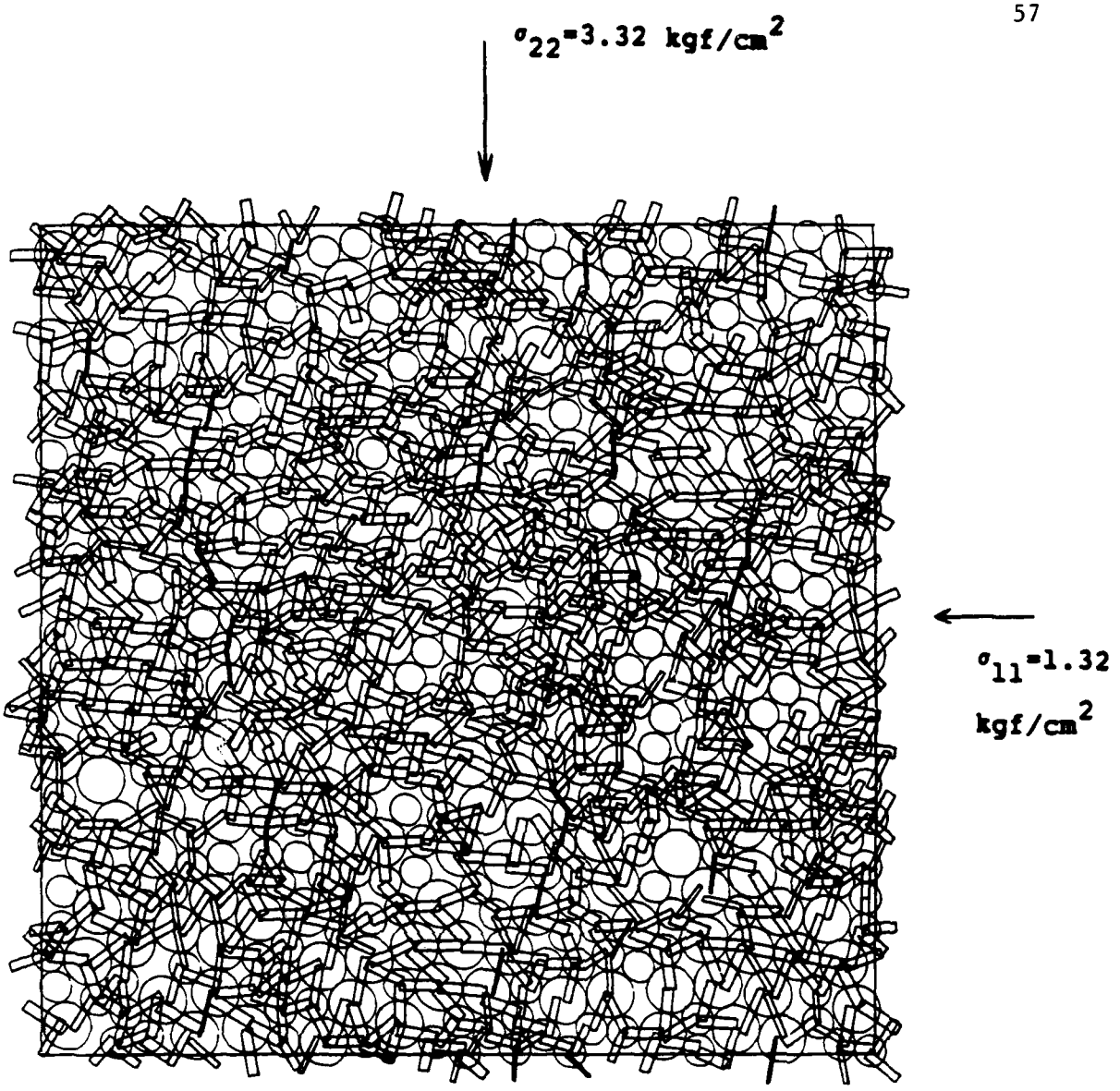

Figure 20. 2-D Random Array of 531 Elastic, Quartz Spheres of Two Radii (R_1/R_2=1.5) Subjected to Biaxial Compression Loading.

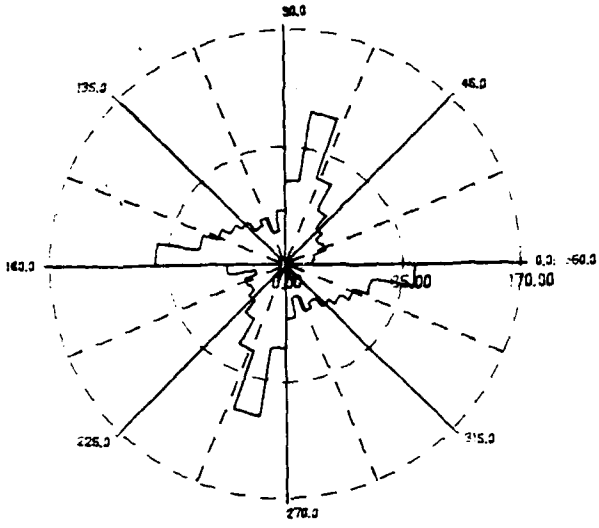

FREQUENCY DISTRIBUTION
OF CONTACT ANGLE

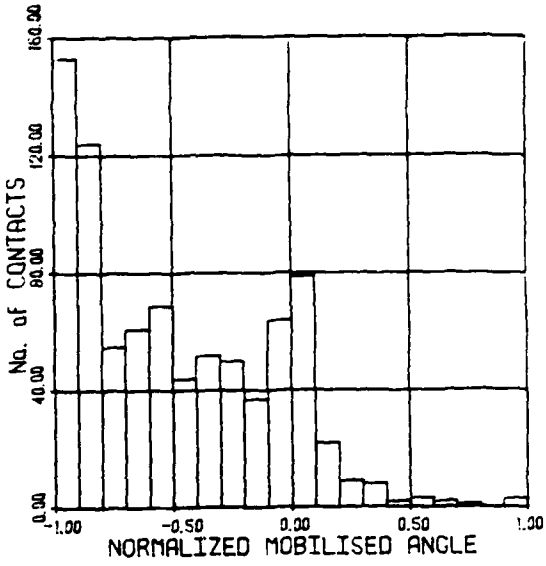

FREQUENCY DISTRIBUTION
OF MOBILISED ANGLE

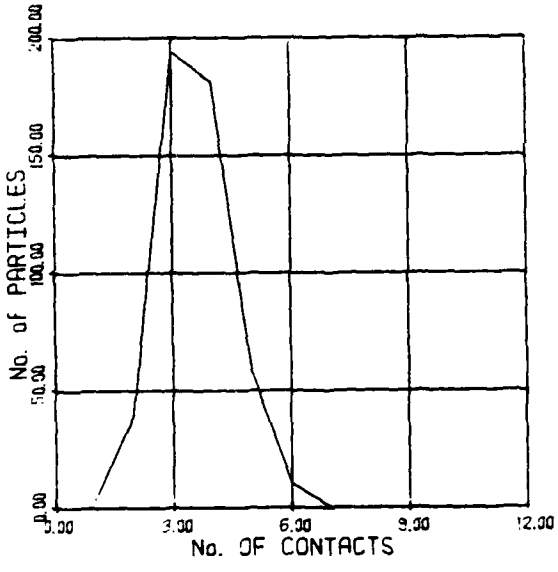

FREQUENCY DISTRIBUTION
OF CONTACT PER PARTICLE

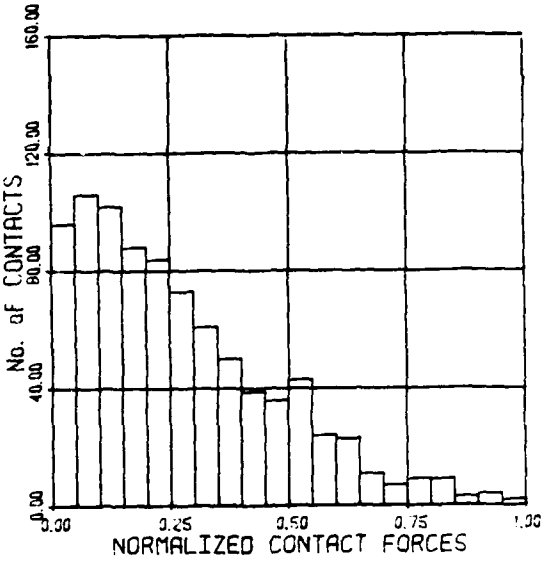

FREQUENCY DISTRIBUTION
OF CONTACT FORCE

Figure 21. Statistical Information for the Biaxial Loading in Figure 20.

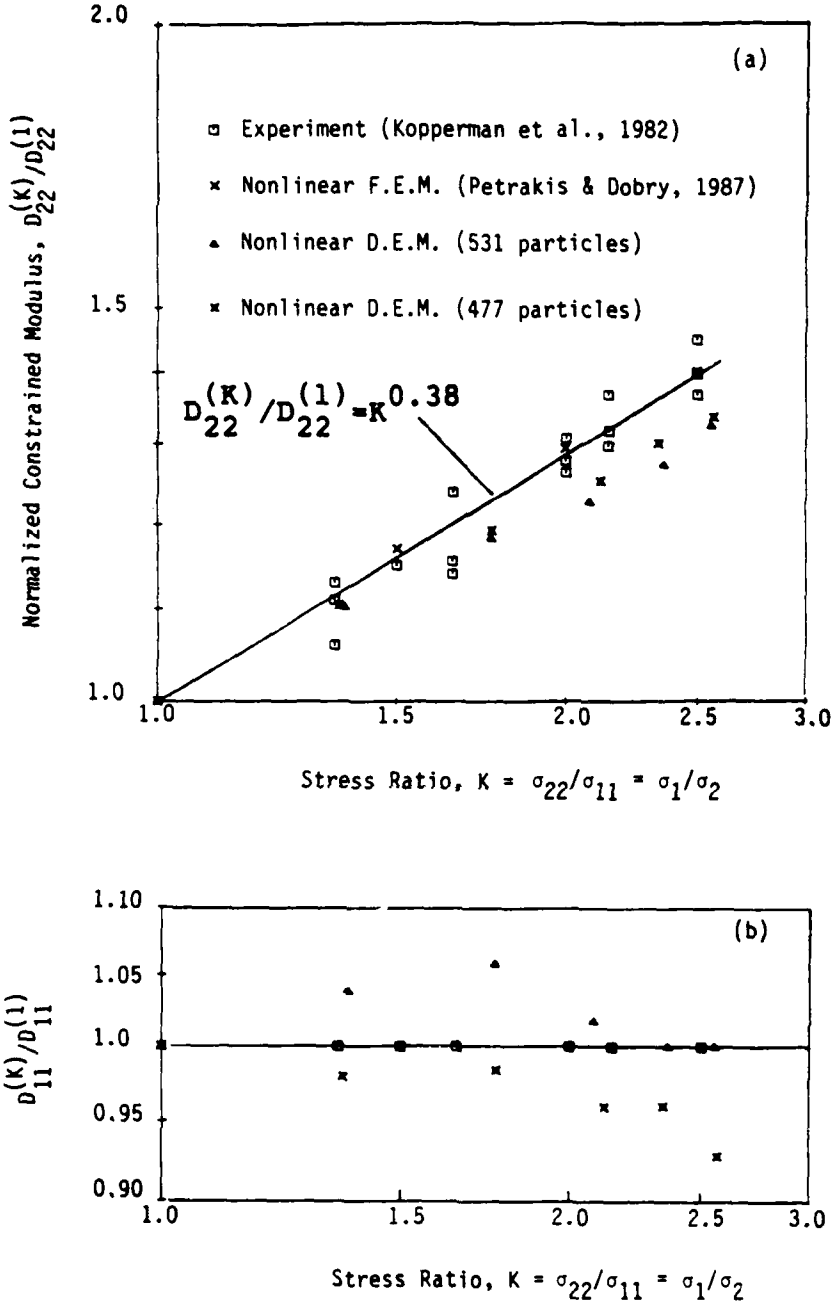

Figure 22. Normalized Constrained Moduli, $D_{ii}^{(K)}/D_{ii}^{(1)}$, Versus Stress Ratio, $K=\sigma_1/\sigma_2 = \sigma_{22}/\sigma_{11}$ All Distinct Element, Finite Element and Experimental Results. (a) In the Direction of σ_{22}, and (b)in the Direction of σ_{11} (σ_{11} is kept constant).